

SPARSE AUTOENCODERS REVEAL UNIVERSAL FEATURE SPACES ACROSS LARGE LANGUAGE MODELS

Michael Lan*

Philip Torr[†] Austin Meek[§] Ashkan Khakzar[‡] David Krueger[♡]

Fazl Barez^{†‡}

[†]Tangentic [‡]University of Oxford [§]University of Delaware [♡]MILA

ABSTRACT

We investigate feature universality in large language models (LLMs), a research field that aims to understand how different models similarly represent concepts in the latent spaces of their intermediate layers. Demonstrating feature universality allows discoveries about latent representations to generalize across several models. However, comparing features across LLMs is challenging due to polysemanticity, in which individual neurons often correspond to multiple features rather than distinct ones. This makes it difficult to disentangle and match features across different models. To address this issue, we employ a method known as *dictionary learning* by using sparse autoencoders (SAEs) to transform LLM activations into more interpretable spaces spanned by neurons corresponding to individual features. After matching feature neurons across models via activation correlation, we apply representational space similarity metrics on SAE feature spaces across different LLMs. Our experiments reveal significant similarities in SAE feature spaces across various LLMs, providing new evidence for feature universality ¹.

1 INTRODUCTION

Large language models (LLMs) have demonstrated remarkable capabilities across a wide range of natural language tasks (Bubeck et al., 2023; Naveed et al., 2024; Liu et al., 2023). However, understanding how these models represent and process information internally remains a significant challenge (Bereska & Gavves, 2024). A key question in this domain is whether different LLMs learn similar internal representations, or if each model develops its own unique way of encoding linguistic knowledge. This question of feature universality is crucial for several reasons: it impacts the generalizability of interpretability findings across models, it could accelerate the development of more efficient training techniques, and it may provide insights into safer and more controllable AI systems (Chughtai et al., 2023b; Gurnee et al., 2024; Sharkey et al., 2024; Bricken et al., 2023).

Comparing features across LLMs is inherently difficult due to the phenomenon of polysemanticity, where individual neurons often correspond to multiple features rather than distinct ones (Elhage et al., 2022). This superposition of features makes it challenging to disentangle and match feature representations across different models. To address these challenges, we propose a novel approach leveraging sparse autoencoders (SAEs) to transform LLM activations into more interpretable spaces before matching features. SAEs allow us to decompose the complex, superposed representations within LLMs into features that correspond to distinct semantic concepts that are easier to analyze and compare across models (Makhzani & Frey, 2013; Cunningham et al., 2023; Bricken et al., 2023). We then apply representational space similarity metrics to these SAE features, enabling a rigorous quantitative analysis of feature universality across different LLMs (Klabunde et al., 2023). Our methodology involves several key steps: obtaining SAEs trained on the activations of multiple LLMs

*Work done during the ERA-Krueger AI Safety Lab internship.
Author contributions detailed in §6.

¹Code for experiments is available at: https://github.com/wlg1/univ_feat_geom

to extract interpretable features, developing and applying representational similarity metrics tailored for high-dimensional SAE feature spaces, and conducting extensive experiments comparing SAE features across models with varying architectures, sizes, and training regimes.

To verify the effectiveness of our approach, we present a comprehensive set of experiments and results. Our experimental approach involves solving two issues for representational space similarity measurement: the permutation issue, which involves aligning individual neurons, and the rotational issue, which involves comparing two spaces which have different basis that are rotationally-invariant. Additionally, we present an approach to filter out feature matches with low semantically-meaningful similarity.

We demonstrate high correlations between individual SAE features extracted from distinct models, providing evidence for feature universality. Furthermore, we show that semantically meaningful subspaces (e.g., features related to specific concepts, such as Emotions) exhibit even higher similarity across models. We also analyze how feature similarity varies across different layers of LLMs, revealing patterns in how representations evolve through the model depth. Lastly, we examine our results to note the differences which are not captured by SAEs. While we discover evidence that LLMs learn weakly universal features, and that SAEs can capture both these features and these relations, we also find that different SAEs do not consistently learn the same universal features captured by LLMs, a finding that is supported by previous work (Leask et al., 2025). Thus, our research guides future work to improve upon methods that can better capture universal representations of features (Thasarathan et al., 2025), and contributes to ongoing research that aims to improve SAEs (Engels et al., 2024b).

This work opens up several exciting avenues for future research. Exploring whether universal features can be leveraged to improve transfer learning or model compression techniques may lead to more efficient training paradigms (Yosinski et al., 2014; Hinton et al., 2015). Additionally, examining the implications of feature universality for AI safety and control, particularly in identifying and mitigating potentially harmful representations, could contribute to the development of safer AI systems (Hendrycks et al., 2023). By shedding light on the internal representations of LLMs, our research contributes to the broader goal of developing more interpretable, efficient, and reliable AI systems (Barez et al., 2023). Understanding the commonalities and differences in how various models encode information is a crucial step toward building a more comprehensive theory of how large language models process and generate human language. **Our key contributions include:**

1. A novel framework for comparing LLM representations using SAEs and similarity metrics.
2. Empirical evidence supporting the existence of universal features across diverse LLMs.
3. A quantitative analysis of how feature similarity varies across layers and semantic domains.
4. A step-by-step approach to compare feature weight representations by paired features that differs from previous methods which compare feature activations.

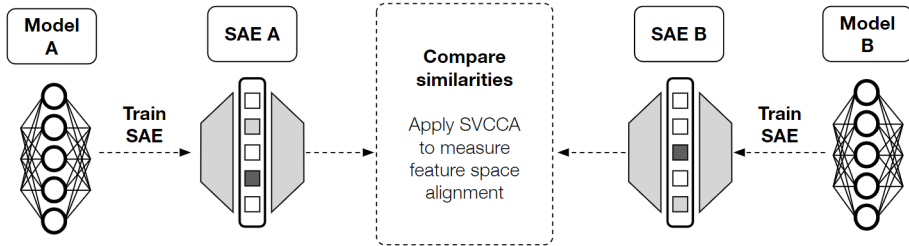


Figure 1: We train SAEs on LLMs, and then compare their SAE feature space similarity using metrics such as Singular Value Canonical Correlation Analysis (SVCCA).

2 BACKGROUND

Feature Universality. Previous studies have explored the concept of universality using various definitions Bricken et al. (2023); Chughtai et al. (2023a). In this paper, we examine universality

through the lens of two definitions: *analogous features* (Olah et al., 2020), and *representational universality* (Gurnee et al., 2024). We define *correlated features* as features which are correlated in terms of activation similarity, and thus activate highly on the same tokens. We measure the *representational universality* of feature spaces by comparing their correlated feature pairs. Correlated features that reside in spaces with notable representational similarity are deemed as *analogous*. Further discussion of these definitions is provided in Appendix §H.

Sparse Autoencoders. Sparse autoencoders (SAEs) are a type of autoencoder designed to learn efficient, sparse representations of input data by imposing a sparsity constraint on the hidden layer (Makhzani & Frey, 2013). The network takes in an input $\mathbf{x} \in \mathbb{R}^n$ and reconstructs it as an output $\hat{\mathbf{x}}$ using the equation $\hat{\mathbf{x}} = \mathbf{W}'\sigma(\mathbf{W}\mathbf{x} + \mathbf{b})$, where $\mathbf{W} \in \mathbb{R}^{h \times n}$ is the encoder weight matrix, \mathbf{b} is a bias term, σ is a nonlinear activation function, and \mathbf{W}' is the decoder matrix, which often uses the transpose of the encoder weights. SAE training aims to both encourage sparsity in the activations $\mathbf{h} = \sigma(\mathbf{W}\mathbf{x} + \mathbf{b})$ and to minimize the reconstruction loss $\|\mathbf{x} - \hat{\mathbf{x}}\|_2^2$.

The sparsity constraint encourages a large number of the neuron activations to remain inactive (close to zero) for any given input, while a few neurons, called *feature neurons*, are highly active. Recent work has replaced the regularization term by using the TopK activation function as the nonlinear activation function, which selects only the top K feature neurons with the highest activations (Gao et al., 2024), zeroing out the other activations. The active feature neurons tend to activate only for specific concepts in the data, promoting monosemanticity. Therefore, since there is a mapping from LLM neurons to SAE feature neurons that "translates" LLM activations to features, this method is a type of *dictionary learning* (Olshausen & Field, 1997).

SAE Feature Weight Spaces. By analyzing UMAPs of feature weights from an SAE trained on a middle residual stream layer of Claude 3 Sonnet, researchers discovered SAE feature spaces organized in neighborhoods of semantic concepts, allowing them to identify subspaces corresponding to concepts such as biology and conflict (Templeton et al., 2024). Additionally, these concepts appear to be organized in hierarchical clusters, such as "disease" clusters that contain sub-clusters of specific diseases like flus. In Section §4.3, we measure the extent of similarity of these semantic feature spaces across LLMs.

Representational Space Similarity. Representational similarity measures typically compare neural network activations by assessing the similarity between activations from a consistent set of inputs (Klabunde et al., 2023). In this paper, we take a different approach by comparing the representations using the decoder weight matrices W' of SAEs, where the columns correspond to the feature neurons. We calculate a similarity score $m(W, W')$ for pairs of representations W in SAE A and W' from SAE B . We obtain two scores via the following two representational similarity metrics:

Singular Value Canonical Correlation Analysis (SVCCA): Canonical Correlation Analysis (CCA) seeks to identify pairs of canonical variables, \mathbf{u}_i and \mathbf{v}_i , from two sets of variables, $\mathbf{X} \in \mathbb{R}^{n \times d_1}$ and $\mathbf{Y} \in \mathbb{R}^{n \times d_2}$, that are maximally correlated with each other (Hotelling, 1936). Singular Value Canonical Correlation Analysis (SVCCA) (Raghu et al., 2017) enhances CCA by first applying Singular Value Decomposition (SVD) to both \mathbf{X} and \mathbf{Y} , which can be expressed as:

$$\mathbf{X} = \mathbf{U}_X \mathbf{S}_X \mathbf{V}_X^T, \quad \mathbf{Y} = \mathbf{U}_Y \mathbf{S}_Y \mathbf{V}_Y^T$$

where \mathbf{U}_X and \mathbf{U}_Y are the matrices containing the left singular vectors (informative directions), and \mathbf{S}_X and \mathbf{S}_Y are diagonal matrices containing the singular values. By projecting the original data onto these informative directions, noise is reduced. SVCCA then applies CCA on the transformed datasets, \mathbf{U}_X and \mathbf{U}_Y , resulting in correlation scores between the most informative components. These scores are averaged to obtain a similarity score.

Representational Similarity Analysis (RSA): Representational Similarity Analysis (RSA) (Kriegeskorte et al., 2008) works by first computing, for each space, a Representational Dissimilarity Matrix (RDM) $\mathbf{D} \in \mathbb{R}^{n \times n}$, where each element of the matrix represents the dissimilarity (or similarity) between every pair of data points within a space. The RDM essentially summarizes the pairwise distances between all possible data pairs in the feature space. A common distance metric used is the Euclidean distance. After an RDM is computed for each space, a correlation measurement like *Spearman's rank correlation coefficient* is applied to the pair of RDMs to obtain a similarity

score. RSA has been applied to measure relational similarity of stimuli across brain regions and of activations across neural network layers (Klabunde et al., 2023).

SVCCA vs RSA. SVCCA focuses on the comparison of entire vector spaces by aligning the principal components (singular vectors) of two representation spaces and then computing the canonical correlations between them. In other words, it identifies directions in the space that carry the most variance and checks how well these align between two models or layers. On the other hand, RSA is primarily concerned with the structure of relationships, or *relational structure*, between different data points (like stimuli) within a representation space. It allows us to measure how well relations such as king-queen transfer across models. Thus, SVCCA focuses on comparing the aligned subspaces of two representation spaces, while RSA is more suitable for analyzing the structural similarity between representations at the level of pairwise relationships.

3 METHODOLOGY

Representational similarity is important for capturing the across-model generalizations of both: 1) Feature Spaces, which are spaces spanned by groups of features, and 2) Feature Relations. We compare SAEs trained on layer A_i from LLM A and layer B_j from LLM B . This is done for every layer pair. To compare latent spaces using our selected metrics, we have to solve both permutation and rotational alignment issues. For the permutation issue, we have to find a way to pair neuron weights. Typically, these metrics are performed by pairing activation vectors from two models according to common input instances. For example, input I_k is passed through models A and B , and then a vector of N_1 neuron activations from model A is compared to a paired vector of N_2 activations from model B . The common input instance creates individual mappings from one space to another, which is required for metrics like SVCCA and RSA (Klabunde et al., 2023).

In our paper, we do not pair activation vectors by input instances, but we pair the feature neuron weights themselves. This means we have to find individual pairings of "similar" neurons in SAE A to SAE B . However, we do not know which features map to which features; the order of these features are permuted in the weight matrices, and some features may not have a corresponding partner. Therefore, we have to pairwise match them via a correlation metric. For the rotational issue, models typically develop their own basis for latent space representations, so features may be similar relation-wise across spaces, but not rotation-wise due to differing basis. To solve this issue, we employ rotation-invariant metrics.

Assessing Scores with Baseline. We follow the approach of Kriegeskorte et al. (2008) to randomly pair features to obtain a baseline score. We compare the score of the features paired by correlation (which we refer to as the "paired features") with the average score of N runs of randomly paired features to obtain a p-value score. If the p-value is less than 0.05, the metric suggests that the similarity is statistically meaningful.

In summary, the steps to carry out our similarity comparison experiments are given below, and steps 1 to 3 are illustrated in Figure 19:

1. For the permutation issue: Get activation correlations for every feature pair from two decoder SAEs for similar LLMs. Pair each feature from model A with its highest activation correlated feature from model B .
2. Rearrange the order of features in each matrix to pair them row by row.
3. For the rotational issue: Apply various rotation-invariant metrics to get a *Paired Score*.
4. Using the same metrics, obtain the similarity scores of N *random pairings* to estimate a null distribution. Obtain a p-value of where the paired score falls in the null distribution to determine statistical significance.

Semantic Subspace Matching Experiments. For these experiments, we first identify semantically similar subspaces, and then compare their similarity. This is summarized by the following steps:

1. We find a group of related features in each model by searching for features which highly activate on the top 5 samples' tokens that belong to a *concept category*. For example, the concept of "emotions" contains keywords such as "rage". Since the correlations are

-
- calculated by tokens, we use single-token keywords. If a keyword from a concept appears at least once, that feature is included. The keywords in each category are given in Appendix L.
 - We obtain mappings between these subsets of features using max activation correlation.
 - We characterize the relationships of features within these groups (eg. pairwise differences between features), and compare these relationships across models using similarity metrics.

Assessing Scores with Baseline. We use two types of tests which compare the paired score to a null distribution. Each test examines that the score is rare under a certain null distribution assumption:

- Test 1: We compare the score of a semantic subspace mapping to the mean score of randomly shuffled pairings of the same subspaces. This test shows just comparing the subspace of features is not enough; the features must be paired.
- Test 2: We compare the score of a semantic subspace mapping to a mean score of mappings between randomly selected feature subsets of the same sizes as the semantic subspaces. This uses a correlation matrix only between the two subsets, not between the entire space. This shows that the high similarity score does not hold for any two subspaces of the same size.

Metrics for the Permutation Issue: These metrics measure individual, local similarity.

Highest Activation Correlation. We take the activation correlations between every feature, following the approach of [Bricken et al. \(2023\)](#). We pass a dataset of samples through both models. Then, for each feature in model *A*, we find its activation correlation with every feature in model *B*, using tokens as the common instance pairing. Lastly, for each feature in model *A*, we find its highest correlated feature in model *B* (as this allows for many-to-1 mappings, this is termed *1A-to-ManyB*; the other way around is *ManyA-to-1B*). We pair these features together when conducting our experiments. We refer to scores obtained by pairing via highest activation correlation as *Paired Scores*.

Filter by Top Tokens. We notice that there are many "non-concept mappings" with "non-concept features" that have top 5 token activations on end-of-text / padding tokens, spaces, new lines, and punctuation; these non-concept mappings greatly bring our scores down as they are not accurately pairing features representing concepts, as we describe further in Appendix K. By filtering max activation correlation mappings to remove non-concept mapping features, we significantly raise the similarity scores. We also only keep mappings that share at least one keyword in their top 5 token activations. The list of non-concept keywords is given in the Appendix K.

Filter Many-to-1 Mappings. We find that some of these mappings are many-to-1, which means that more than one feature maps to the same feature. We found that removing many-to-1 mappings slightly increased the scores, and we discuss possible reasons why this may occur in Appendix J. However, the scores still show high similarity even with the inclusion of many-to-1 mappings, as seen in Figures 2. We show only scores of 1-to-1 mappings (filtering out the many-to-1 mappings) in the main text, and show scores of many-to-1 mappings in Appendix J. We use features from the SAEs of Pythia-70m and Gemma-1-2B as "many" features which map onto "one" feature in the SAEs of Pythia-160m and Gemma-2-2B.

Metrics for the Rotational Issue: Rotation-invariant metrics measure global similarity after feature pairing. We apply metrics which measure: 1) How well subspaces align using **SVCCA**, and 2) How similar feature relations like king-queen are using **RSA**. We set the inner similarity function using Pearson correlation the outer similarity function using Spearman correlation, and compute the RDM using Euclidean Distance.

4 EXPERIMENTS

4.1 EXPERIMENTAL SETUP

LLM Models. We compare LLMs that use the Transformer model architecture ([Vaswani et al., 2017](#)). We compare models that use the same tokenizer because the highest activation correlation pairing relies on comparing two activations using the same tokens. We compare the residual streams of Pythia-70m, which has 6 layers and 512 dimensions, to Pythia-160m, which has 12 layers and 768 dimensions ([Biderman et al., 2023](#)). We compare the residual streams of Gemma-1-2B, which has 18 layers and 2048 dimensions, to Gemma-2-2B, which has 26 layers and 2304 dimensions ([Team](#)

et al., 2024a;b).² We compare SAEs trained on the same Tinystories model (Eldan & Li, 2023) in Appendix §E, and show results for across Llama 3 and 3.1 models (Dubey et al., 2024; AI, 2024) in Appendix §C.3. In total, we compare 5 model pairs and find notable similarities across their SAEs. The list of model pairs is given in Appendix A.

SAE Models. For Pythia, we use pretrained SAEs with 32768 feature neurons trained on residual stream layers from Eleuther (EleutherAI, 2023). For Gemma, we use pretrained SAEs with 16384 feature neurons trained on residual stream layers (Lieberum et al., 2024) We access pretrained Gemma-1-2B SAEs for layers 0, 6, 10, 12, and 17, and Gemma-2-2B SAEs for layers 0 to 26, through the SAELens library (Bloom & Chanin, 2024).

In Appendix §C, we compare SAEs for Gemma-2-2B vs Gemma-2-9B, base vs fined tuned versions for Gemma-2-9B vs Gemma-2-9B-Instruct and Gemma-1-2B vs Gemma-1-2B-Instruct (at Layer 12), and for Llama 3-8B and Llama 3.1-8B (at Layer 25). The list of all models used in experiments is provided in Section §A. In Appendix §D, we assess a baseline comparison that compares Pythia-70m SAEs with SAEs trained on a randomized Pythia-70m. In Appendix §E, we compare SAEs trained within the same model. Lastly, in Appendix §F, we compare SAEs across Pythia-70m and Pythia-160m as we vary SAE widths.

Datasets. We obtain SAE activations using OpenWebText, a dataset that scraps internet content (Gokaslan & Cohen, 2019). We use 100 samples with a max sequence length of 300 for Pythia for a total of 30k tokens, and we use 150 samples with a max sequence length of 150 for Gemma for a total of 22.5k tokens. Top activating dataset tokens were also obtained using OpenWebText samples. In Appendix §G, we vary the dataset and number of tokens used to obtain activations to show that our results do not drastically change when these factors are varied.

Computing Resources. We run experiments on an A100 GPU.

4.2 SAE SPACE SIMILARITY

In summary, for almost all layer pairs after layer 0, we find the p-value of SAE experiments for SVCCA, which measures rotationally-invariant alignment, to be low; all of them are between 0.00 to 0.01 using 100 samples.³ While RSA also passes many p-value tests, their values are much lower, suggesting a relatively weaker similarity in terms of pairwise differences. It is possible that many features are not represented in just one layer; hence, a layer from one model can have similarities to multiple layers in another model. We also note that the first layer of every model, layer 0, has a very high p-value when compared to every other layer, including when comparing layer 0 from another model. This may be because layer 0 contains few discernible, meaningful, and comparable features.

As shown in Figure 24 for Pythia and Figure 25 for Gemma in Appendix M, we also find that mean of the highest activation correlations does not always correlate with the global similarity metric scores. For instance, a subset of feature pairings with a moderately high mean activation correlation (eg. 0.6) may yield a low SVCCA score (eg. 0.03).

Because LLMs, even with the same architecture, can learn many different features, we do not expect entire feature spaces to be highly similar; instead, we hypothesize there may be highly similar *subspaces*. In other words, there are many similar features universally found across SAEs, but not every feature learned by different SAEs is the same. Our experimental results support this hypothesis.

Pythia-70m vs Pythia-160m . In Figure 20, we compare Pythia-70m, which has 6 layers, to Pythia-160m, which has 12 layers. When compared to Figures 26 and 27 in Appendix M, for all layers pairs (excluding Layers 0), and for both SVCCA and RSA scores, almost all the p-values of the residual stream layer pairs are between 0% to 1%, indicating that the feature space similarities are statistically meaningful. In particular, Figure 20 shows that Layers 2 and 3, which are middle layer of Pythia-70m, are more similar by SVCCA and RSA scores to middle layers 4 to 7 of Pythia-160m compared to other layers. Figure 20 also shows that Layer 5, the last residual stream layer of Pythia-70m, is more similar to later layers of Pythia-160m than to other layers. The number of features after filtering non-concept features and many-to-1 features are given in Tables 5 and 6 in Appendix M.

²Gemma-2 introduces several architectural improvements over Gemma-1 (Team et al., 2024a;b).

³Only 100 samples were used as we found the variance to be low for the null distribution, and that the mean was similar for using 100 vs 1k samples.

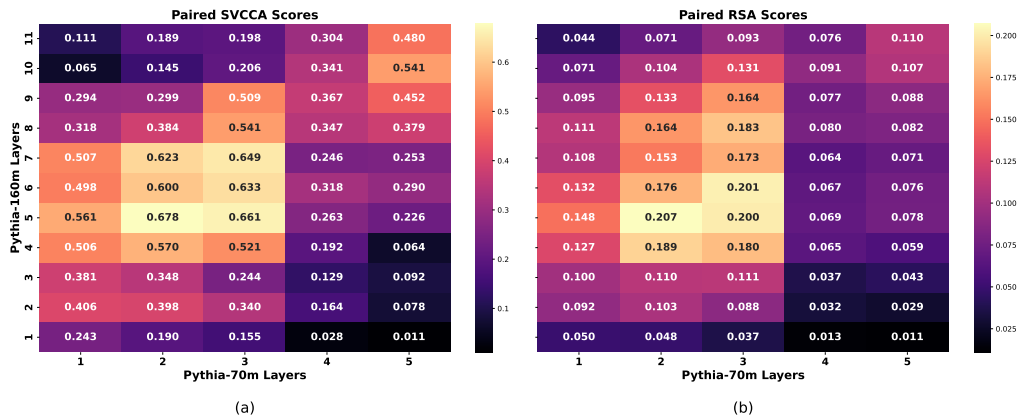


Figure 2: (a) SVCCA and (b) RSA 1-1 paired scores of SAEs for layers in Pythia-70m vs layers in Pythia-160m. We find that middle layers have the most similarity with one another (as shown by the high-similarity block spanned by layers 1 to 3 in Pythia-70m and Layers 4 to 7 in Pythia-160m). We exclude layers 0, as we observe they always have non-statistically significant similarity. The 1-1 scores are slightly higher for most of the Many-to-1 scores shown in Figure 20, and the SVCCA score at L2 vs L3 for 70m vs 160m is much higher.

Gemma-1-2B vs Gemma-2-2B. As shown by the paired SVCCA and RSA results for these models in Figure 22, we find that using SAEs, we can detect highly similar features in layers across Gemma-1-2B and Gemma-2-2B. Compared to mean random pairing scores and p-values in Figures 28 and 29 in Appendix M, for all layers pairs (excluding Layers 0), and for both SVCCA and RSA scores, almost all the p-values of the residual stream layer pairs are between 0% to 1%, indicating that the feature space similarities are statistically meaningful. The number of features after filtering non-concept features and many-to-1 features are given in Tables 7 and 8 in Appendix M.

Rather than just finding that middle layers are more similar to middle layers, we also find that they are the best at representing concepts. This is consistent with work by (Rimsky et al., 2024), which find the best steering vectors in middle layers for steering behaviors such as sycophancy. Other papers find that middle layers tend to provide better directions for eliminating refusal behavior (Arditi et al., 2024) and work well for representing goals and finding steering vectors in policy networks (Mini et al., 2023). In fact, we find that early layers do not represent universal features well, perhaps due to lacking content, while later layers do not represent them as well as middle layers, perhaps due to being too specific/complex.

4.3 SIMILARITY OF SEMANTICALLY MATCHED SAE FEATURE SPACES

We find that for all layers and for all concept categories, Test 2 described in §3 is passed. Thus, we only report specific results for Test 1 in Tables 1 and 2. Overall, in both Pythia and Gemma models and for many concept categories, we find that semantic subspaces are more similar to one another than non-semantic subspaces.

Pythia-70m vs Pythia-160m. We compare every layer of Pythia-70m to every layer of Pythia-160m for several concept categories. While many layer pairs have similar semantic subspaces. Middle layers appear to have the semantic subspaces with the highest similarity. Table 1 demonstrates one example of this by comparing the SVCCA score for layer 3 to layer 5 of Pythia-160m, which shows high similarity for semantic subspaces across models, as the concept categories all pass Test 1, having p-values below 0.05. We show the scores for other layer pairs and categories in Figures 30 and 32 in Appendix M, which include RSA scores in Table 9.

Gemma-1-2B vs Gemma-2-2B. In Table 2, we compare L12 of Gemma-1-2B vs L14 of Gemma-2-2B. As shown in Figure 22, this layer pair has a very high similarity for most concept spaces; as such, they likely have high similar semantically-meaningful feature subspaces. Notably, not all concept group are not highly similar; for instance, unlike in Pythia, the Country concept group does not pass

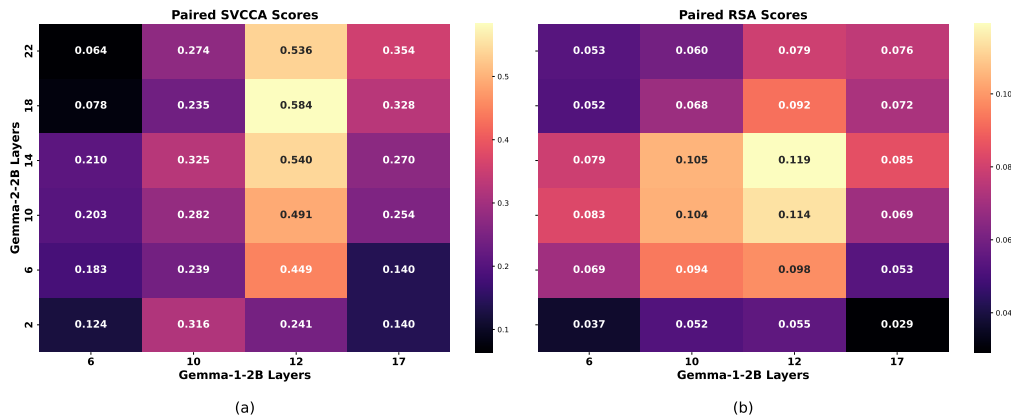


Figure 3: (a) SVCCA and (b) RSA 1-1 paired scores of SAEs for layers in Gemma-1-2B vs layers in Gemma-2-2B. Middle layers have the best performance. The later layer 17 in Gemma-1 is more similar to later layers in Gemma-2. Early layers like Layer 2 in Gemma-2 have very low similarity. We exclude layers 0, as we observe they always have non-statistically significant similarity. The 1-1 scores are slightly higher for most of the Many-to-1 scores shown in Figure 22.

Table 1: SVCCA scores and random mean results for 1-1 semantic subspaces of L3 of Pythia-70m vs L5 of Pythia-160m. P-values are taken for 1000 samples in the null distribution.

Concept Subspace	Number of Features	Paired Mean	Random Shuffling Mean	p-value
Time	228	0.59	0.05	0.00
Calendar	126	0.65	0.07	0.00
Nature	46	0.50	0.12	0.00
Countries	32	0.72	0.14	0.00
People/Roles	31	0.50	0.15	0.00
Emotions	24	0.83	0.15	0.00

the Test 1 as it has a p-value above 0.05. We show the scores for other layer pairs and categories in Figures 34 and 36 in Appendix M.

5 RELATED WORK

Superposition and Sparse Autoencoders. Superposition is a phenomenon in which a model, in response to the issue of having to represent more features than it has parameters, learns feature representations distributed across many parameters (Elhage et al., 2022). This causes its parameters, or neurons, to be polysemantic, which means that each neuron is involved in representing more than one feature. This leads to issues for interpretability, which aims to disentangle and cleanly identify

Table 2: SVCCA scores and random mean results for 1-1 semantic subspaces of L12 of Gemma-1-2B vs L14 of Gemma-2-2B. P-values are taken for 1000 samples in the null distribution.

Concept Subspace	Number of Features	Paired SVCCA	Random Shuffling Mean	p-value
Time	228	0.46	0.06	0.00
Calendar	105	0.54	0.07	0.00
Nature	51	0.30	0.11	0.01
Countries	21	0.39	0.17	0.07
People/Roles	36	0.66	0.15	0.00
Emotions	35	0.60	0.12	0.00

features in models in order to manipulate them, such as by steering a model away from deception (Templeton et al., 2024). To address the issue of polysemanticity, Sparse Autoencoders (SAEs) have been applied to disentangle an LLM’s polysemantic neuron activations into monosemantic "feature neurons", which are encouraged to represent an isolated concept (Makhzani & Frey, 2013; Cunningham et al., 2023; Gao et al., 2024; Rajamanoharan et al., 2024a;b). Features interactions in terms of circuits have also been studied (Marks et al., 2024).

Feature Universality. To the best of our knowledge, only Bricken et al. (2023) has done a quantitative study on individual SAE feature similarity for two 1-layer toy models, finding that individual SAE feature correlations are stronger than individual LLM neuron correlations; however, this study did not analyze the global properties of feature spaces. Gurnee et al. (2024) found evidence of universal neurons across language models by applying pairwise correlation metrics, and taxonomized families of neurons based on patterns of downstream, functional effects. O’Neill et al. (2024) discover "feature families", which represent related hierarchical concepts, in SAEs across two different datasets.

Of note is that our paper seeks to measure the extent of universality in terms of *analogous features* and *representational universality*, as defined in previous work (Olah et al., 2020; Gurnee et al., 2024), but we do not measure *true features*, which are exact, atomic hypothesized ground truth features that models may converge towards capturing. This is explained further in Appendix §H. Recent work has shown that as vision and language models are trained with more parameters and with better methods, their representational spaces converge towards more similar representations (Huh et al., 2024). However, we do not claim nor attempt to study in this paper if models converge towards finding the same features.

Representational Space Similarity. Previous work has studied neuron activation spaces by utilizing metrics to compare the geometric similarities of representational spaces (Raghu et al., 2017; Wang et al., 2018b; Kornblith et al., 2019; Klabunde et al., 2024; 2023; Kriegeskorte et al., 2008; Sucholutsky et al., 2023). It was found that even models with different architectures may share similar representation spaces, hinting at feature universality. However, these techniques have yet to be applied to the feature spaces of sparse autoencoders trained on LLMs. Moreover, these techniques compare the similarity of paired input activations. Our work differs as it compares the similarity of paired *feature weights*. Essentially, previous works do not show that one can match LLMs by features that both LLMs find in common.

Feature Manifolds. In real world data, features may lie on a manifold, where nearby features respond to similar data. (Olah & Batson, 2023; Bricken et al., 2023). Previous work has discovered the existence of features corresponding to months and days of the week arranged in a circular structure in SAE feature spaces across models (Engels et al., 2024a). Studying how feature arrangements generalize across models may shed light on how features lie on a manifold.

Mechanistic Interpretability. Recent work has made notable progress in neuron interpretation (Foote et al., 2023; Garde et al., 2023) and interpreting the interactions between Attention Heads and MLPs (Neo et al., 2024). Other work in mechanistic interpretability has traditionally focused on 'circuits'-style analysis (Elhage et al., 2021), as well as the use of steering vectors to control model behaviors at inference using identified representations (Zou et al., 2023; Turner et al., 2023; Bereska & Gavves, 2024). These approaches have been combined with SAEs to steer models in the more interpretable SAE feature space (Nanda & Conmy, 2024). Steering vectors have been found across models; for instance, Arditi et al. (2024) found "Refusal Vectors" that steered a model to refuse harmful instructions across 13 different models, including Gemma and Llama-2.

AI Safety. Advanced AI systems may not be well aligned with the values of their designers (Ngo et al., 2022), due to phenomena such as goal misgeneralization (Shah et al., 2022; Langosco et al., 2022), deceptive alignment (Hubinger et al., 2024; 2021; Greenblatt et al., 2024), sycophancy (Sharma et al., 2023), and reward tampering (Denison et al., 2024). SAEs may be able to find AI safety-related features across models; using SAEs to reliably find universal capabilities, especially in combination with control methods such as steering Chalnev et al. (2024), may help provide solutions to the above phenomena.

6 CONCLUSION

In this study, we address the underexplored domain of feature universality in sparse autoencoders (SAEs) trained on LLMs with multiple layers and across multiple model pairs. To achieve these insights, we developed a novel methodology to pair features with high mean activation correlations, and then assess their global similarity of the resulting subspaces using SVCCA and RSA. Our findings reveal a high degree of similarity in SAE feature subspaces across various models. Furthermore, our research reveals that subspaces of features associated with specific semantic concepts, such as calendar or people tokens, demonstrate remarkably high similarity across different models. This suggests that certain semantic feature subspaces are universally encoded across varied LLM architectures. However, our results also show that there are parts of SAE feature spaces which do not match, and may suggest that either certain features are not captured universally, or that SAEs have limitations in capturing universal features. We believe that future work can benefit from these discoveries to find better ways on improving methods to capture feature universality. Our work enhances understanding of how LLMs represent information at a fundamental level, opening up new avenues for further research into model interpretability and the transferability of learned features.

LIMITATIONS

We perform analysis only on a sample of SAEs for similar LLMs that use the same tokenizer, and focus on SAEs with the same or similar number of features. As we pair features by activation correlation, we do not perform analysis on models that use different tokenizers. Although, for some examples, we obtain good results when pairing features only by semantic similarity, these results were not consistent when applied to other examples, perhaps due to the lower pairing quality, as the representational similarity metrics depend on the pairing choice. Future work can analyze models whose representations do not depend as much on the tokenizer choice (team et al., 2024).

Our study is also limited by the inherent challenges in interpreting and comparing high-dimensional feature spaces. The methods we used to measure similarity, while robust, may not capture all nuances of feature interactions and representations within the SAEs. Additionally, our analysis is constrained by the computational resources available, which may have limited the scale and depth of our comparisons. The generalizability of our findings to SAEs trained on more diverse datasets or specialized domain-specific LLMs remains an open question. Furthermore, the static nature of our analysis does not account for potential temporal dynamics in feature representation that might occur during the training process of both LLMs and SAEs. Lastly, functional similarity experiments were not examined.

IMPACT STATEMENT

Our study investigates feature universality in large language models (LLMs) using sparse autoencoders (SAEs) to identify common feature spaces across models. This research contributes to safety research by providing insights into how different LLMs encode safety-related concepts, which has several ethical and societal implications. By identifying universal feature spaces, our approach may aid in the detection of harmful or deceptive model behaviors across different architectures. Understanding how models encode knowledge could lead to improved transparency and control mechanisms, reducing risks associated with goal misgeneralization and deceptive alignment in AI systems. Additionally, identifying shared feature structures can inform bias mitigation strategies, as universal features could either amplify or help detect biases present across multiple models.

AUTHOR CONTRIBUTIONS

Michael conceived the study and designed the experiments with help from Fazl. Michael performed the experiments with help from Austin and led the writing of the manuscript. Philp, Ashkan and David provided advice throughout the project. Fazl advised this work and helped significantly with the write-up of the paper.

ACKNOWLEDGMENTS

We thank the Torr Vision Group at the University of Oxford for providing compute and hosting Michael Lan during the internship. We thank Clement Neo, Luke Marks, Minseon Kim, Lovis Heinrich, Tingchen Fu, Constantin Venhoff, Hazel Kim, Will Lin, Alasdair Paren, Christian Schroeder de Witt, Kiho Park, and Max Klabunde for providing helpful feedback. Clement Neo helped with the design of Figure 1.

REFERENCES

- AI, M. Introducing llama 3.1: Our most capable models to date. *AI at Meta*, 2024. URL <https://ai.meta.com/blog/meta-llama-3-1/>.
- Arditi, A., Obeso, O., Syed, A., Paleka, D., Rimsy, N., Gurnee, W., and Nanda, N. Refusal in language models is mediated by a single direction, 2024.
- Barez, F., Hasanbieg, H., and Abbate, A. System iii: Learning with domain knowledge for safety constraints, 2023.
- Bereska, L. and Gavves, E. Mechanistic interpretability for ai safety – a review, 2024. URL <https://arxiv.org/abs/2404.14082>.
- Biderman, S., Schoelkopf, H., Anthony, Q., Bradley, H., O’Brien, K., Hallahan, E., Khan, M. A., Purohit, S., Prashanth, U. S., Raff, E., Skowron, A., Sutawika, L., and van der Wal, O. Pythia: A suite for analyzing large language models across training and scaling, 2023. URL <https://arxiv.org/abs/2304.01373>.
- Bloom, J. and Chanin, D. Saelens. <https://github.com/jbloomAus/SAELens>, 2024.
- Bricken, T., Templeton, A., Batson, J., Chen, B., Jermyn, A., Conerly, T., Turner, N., Anil, C., Denison, C., Askell, A., Lasenby, R., Wu, Y., Kravec, S., Schiefer, N., Maxwell, T., Joseph, N., Hatfield-Dodds, Z., Tamkin, A., Nguyen, K., McLean, B., Burke, J. E., Hume, T., Carter, S., Henighan, T., and Olah, C. Towards monosemanticity: Decomposing language models with dictionary learning. *Transformer Circuits Thread*, 2023. <https://transformer-circuits.pub/2023/monosemantic-features/index.html>.
- Bubeck, S., Chandrasekaran, V., Eldan, R., Gehrke, J., Horvitz, E., Kamar, E., Lee, P., Lee, Y. T., Li, Y., Lundberg, S., Nori, H., Palangi, H., Ribeiro, M. T., and Zhang, Y. Sparks of artificial general intelligence: Early experiments with gpt-4, 2023. URL <https://arxiv.org/abs/2303.12712>.
- Bussmann, B., Pearce, M., Leask, P., Bloom, J. I., Sharkey, L., and Nanda, N. Showing sae latents are not atomic using meta-saes. *AI Alignment Forum*, 2024. URL <https://www.alignmentforum.org/posts/TMAmHh4DdMr4nCSr5/showing-sae-latents-are-not-atomic-using-meta-saes>.
- Chalnev, S., Siu, M., and Conmy, A. Improving Steering Vectors by Targeting Sparse Autoencoder Features, 2024. URL <http://arxiv.org/abs/2411.02193>. arXiv:2411.02193 [cs].
- Chanin, D., Wilken-Smith, J., Dulka, T., Bhatnagar, H., and Bloom, J. A is for absorption: Studying feature splitting and absorption in sparse autoencoders, 2024. URL <https://arxiv.org/abs/2409.14507>.
- Chughtai, B., Chan, L., and Nanda, N. A toy model of universality: reverse engineering how networks learn group operations. In *Proceedings of the 40th International Conference on Machine Learning, ICML’23*. JMLR.org, 2023a.
- Chughtai, B., Chan, L., and Nanda, N. A toy model of universality: Reverse engineering how networks learn group operations, 2023b. URL <https://arxiv.org/abs/2302.03025>.
- Cunningham, H., Ewart, A., Riggs, L., Huben, R., and Sharkey, L. Sparse autoencoders find highly interpretable features in language models, 2023. URL <https://arxiv.org/abs/2309.08600>.

-
- Denison, C., MacDiarmid, M., Barez, F., Duvenaud, D., Kravec, S., Marks, S., Schiefer, N., Soklaski, R., Tamkin, A., Kaplan, J., Shlegeris, B., Bowman, S. R., Perez, E., and Hubinger, E. Sycophancy to Subterfuge: Investigating Reward-Tampering in Large Language Models, June 2024. URL <http://arxiv.org/abs/2406.10162>. arXiv:2406.10162 [cs].
- Ding, Z., Tran, D. T., Ponder, K., Cobos, E., Ding, Z., Fahey, P. G., Wang, E., Muhammad, T., Fu, J., Cadena, S. A., Papadopoulos, S., Patel, S., Franke, K., Reimer, J., Sinz, F. H., Ecker, A. S., Pitkow, X., and Tolia, A. S. Bipartite invariance in mouse primary visual cortex. *bioRxiv*, March 2023. doi: 10.1101/2023.03.15.532836. URL <https://www.biorxiv.org/content/10.1101/2023.03.15.532836v1>. Preprint.
- Dubey, A., Jauhri, A., Pandey, A., et al. The llama 3 herd of models. *arXiv preprint arXiv:2407.21783*, 2024. URL <https://arxiv.org/abs/2407.21783>.
- Eldan, R. Tinstories-1layer-21m. <https://huggingface.co/roneneldan/TinyStories-1Layer-21M>, 2023.
- Eldan, R. and Li, Y. Tinstories: How small can language models be and still speak coherent english?, 2023. URL <https://arxiv.org/abs/2305.07759>.
- EleutherAI. Sparse autoencoders (sae) repository. <https://github.com/EleutherAI/sae>, 2023.
- Elhage, N., Nanda, N., Olsson, C., Henighan, T., Joseph, N., Mann, B., Askell, A., Bai, Y., Chen, A., Conerly, T., DasSarma, N., Drain, D., Ganguli, D., Hatfield-Dodds, Z., Hernandez, D., Jones, A., Kernion, J., Lovitt, L., Ndousse, K., Amodei, D., Brown, T., Clark, J., Kaplan, J., McCandlish, S., and Olah, C. A mathematical framework for transformer circuits. *Transformer Circuits Thread*, 2021. <https://transformer-circuits.pub/2021/framework/index.html>.
- Elhage, N., Hume, T., Olsson, C., Schiefer, N., Henighan, T., Kravec, S., Hatfield-Dodds, Z., Lasenby, R., Drain, D., Chen, C., Grosse, R., McCandlish, S., Kaplan, J., Amodei, D., Wattenberg, M., and Olah, C. Toy models of superposition. *Transformer Circuits Thread*, 2022. https://transformer-circuits.pub/2022/toy_model/index.html.
- Engels, J., Liao, I., Michaud, E. J., Gurnee, W., and Tegmark, M. Not all language model features are linear, 2024a. URL <https://arxiv.org/abs/2405.14860>.
- Engels, J., Riggs, L., and Tegmark, M. Decomposing the dark matter of sparse autoencoders, 2024b. URL <https://arxiv.org/abs/2410.14670>.
- Foote, A., Nanda, N., Kran, E., Konstas, I., Cohen, S., and Barez, F. Neuron to graph: Interpreting language model neurons at scale, 2023. URL <https://arxiv.org/abs/2305.19911>.
- Gao, L., la Tour, T. D., Tillman, H., Goh, G., Troll, R., Radford, A., Sutskever, I., Leike, J., and Wu, J. Scaling and evaluating sparse autoencoders, 2024. URL <https://arxiv.org/abs/2406.04093>.
- Garde, A., Kran, E., and Barez, F. Deepdecipher: Accessing and investigating neuron activation in large language models, 2023. URL <https://arxiv.org/abs/2310.01870>.
- Gokaslan, A. and Cohen, V. Openwebtext corpus. <http://Skylion007.github.io/OpenWebTextCorpus>, 2019. Accessed: [Insert date you accessed the resource].
- Goldstein, A., Grinstead-Dabush, A., Schain, M., Wang, H., Hong, Z., Aubrey, B., Nastase, S. A., Zada, Z., Ham, E., Feder, A., Gazula, H., Buchnik, E., Doyle, W., Devore, S., Dugan, P., Reichart, R., Friedman, D., Brenner, M., Hassidim, A., Devinsky, O., Flinker, A., and Hasson, U. Alignment of brain embeddings and artificial contextual embeddings in natural language points to common geometric patterns. *Nature Communications*, 15(1):2768, 2024. doi: 10.1038/s41467-024-46631-y.
- Greenblatt, R., Denison, C., Wright, B., Roger, F., MacDiarmid, M., Marks, S., Treutlein, J., Belonax, T., Chen, J., Duvenaud, D., Khan, A., Michael, J., Mindermann, S., Perez, E., Petrini, L., Uesato, J., Kaplan, J., Shlegeris, B., Bowman, S. R., and Hubinger, E. Alignment faking in large language models, 2024. URL <http://arxiv.org/abs/2412.14093>. arXiv:2412.14093 [cs].

-
- Gurnee, W., Horsley, T., Guo, Z. C., Kheirkhah, T. R., Sun, Q., Hathaway, W., Nanda, N., and Bertsimas, D. Universal neurons in gpt2 language models, 2024. URL <https://arxiv.org/abs/2401.12181>.
- Heap, T., Lawson, T., Farnik, L., and Aitchison, L. Sparse autoencoders can interpret randomly initialized transformers, 2025. URL <https://arxiv.org/abs/2501.17727>.
- Hendrycks, D., Mazeika, M., and Woodside, T. An overview of catastrophic ai risks, 2023. URL <https://arxiv.org/abs/2306.12001>.
- Hindupur, S. S. R., Lubana, E. S., Fel, T., and Ba, D. Projecting assumptions: The duality between sparse autoencoders and concept geometry, 2025. URL <https://arxiv.org/abs/2503.01822>.
- Hinton, G. E., Vinyals, O., and Dean, J. Distilling the knowledge in a neural network. *ArXiv*, abs/1503.02531, 2015. URL <https://api.semanticscholar.org/CorpusID:7200347>.
- Hotelling, H. Relations between two sets of variates. *Biometrika*, 28(3/4):321–377, 1936.
- Hubinger, E., van Merwijk, C., Mikulik, V., Skalse, J., and Garrabrant, S. Risks from Learned Optimization in Advanced Machine Learning Systems, December 2021. URL <http://arxiv.org/abs/1906.01820>. arXiv:1906.01820 [cs].
- Hubinger, E., Denison, C., Mu, J., Lambert, M., Tong, M., MacDiarmid, M., Lanham, T., Ziegler, D. M., Maxwell, T., Cheng, N., Jermyn, A., Askell, A., Radhakrishnan, A., Anil, C., Duvenaud, D., Ganguli, D., Barez, F., Clark, J., Ndousse, K., Sachan, K., Sellitto, M., Sharma, M., DasSarma, N., Grosse, R., Kravec, S., Bai, Y., Witten, Z., Favaro, M., Brauner, J., Karnofsky, H., Christiano, P., Bowman, S. R., Graham, L., Kaplan, J., Mindermann, S., Greenblatt, R., Shlegeris, B., Schiefer, N., and Perez, E. Sleeper Agents: Training Deceptive LLMs that Persist Through Safety Training, January 2024. URL <http://arxiv.org/abs/2401.05566>. arXiv:2401.05566 [cs].
- Huh, M., Cheung, B., Wang, T., and Isola, P. The platonic representation hypothesis, 2024.
- Karvonen, A., Rager, C., Lin, J., Tigges, C., Bloom, J., Chanin, D., Lau, Y.-T., Farrell, E., Conmy, A., McDougall, C., Ayonrinde, K., Wearden, M., Marks, S., and Nanda, N. Saebench: A comprehensive benchmark for sparse autoencoders, 2024. URL <https://www.neuronpedia.org/sae-bench/info>. Accessed: March 12, 2025.
- Kissane, C., Krzyzanowski, R., Conmy, A., and Nanda, N. SAEs (usually) Transfer Between Base and Chat Models, 2024a. URL <https://www.lesswrong.com/posts/fmwk6qxrPw8d4jvbd/saes-usually-transfer-between-base-and-chat-models>. Accessed: 2025-03-15.
- Kissane, C., robertzk, Nanda, N., and Conmy, A. Saes are highly dataset dependent: a case study on the refusal direction, November 2024b. URL <https://www.lesswrong.com/posts/rtp6n7Z23uJpEH7od/saes-are-highly-dataset-dependent-a-case-study-on-the-refusal-direction>. LessWrong post; accessed March 12, 2025.
- Klabunde, M., Schumacher, T., Strohmaier, M., and Lemmerich, F. Similarity of neural network models: A survey of functional and representational measures, 2023. URL <https://arxiv.org/abs/2305.06329>.
- Klabunde, M., Wald, T., Schumacher, T., Maier-Hein, K., Strohmaier, M., and Lemmerich, F. Resi: A comprehensive benchmark for representational similarity measures, 2024. URL <https://arxiv.org/abs/2408.00531>.
- Kornblith, S., Norouzi, M., Lee, H., and Hinton, G. Similarity of neural network representations revisited, 2019. URL <https://arxiv.org/abs/1905.00414>.
- Kriegeskorte, N., Mur, M., and Bandettini, P. Representational similarity analysis – connecting the branches of systems neuroscience. *Frontiers in Systems Neuroscience*, 2:4, 2008. doi: 10.3389/neuro.06.004.2008. URL <https://www.frontiersin.org/articles/10.3389/neuro.06.004.2008/full>.

-
- Kutsyk, T., Mencattini, T., and Florea, C. Do sparse autoencoders (saes) transfer across base and finetuned language models?, sep 2024. URL <https://www.lesswrong.com/posts/bsXPTiAhhwt5nwBW3/do-sparse-autoencoders-saes-transfer-across-base-and>. LessWrong post; accessed March 12, 2025.
- Langosco, L. L. D., Koch, J., Sharkey, L. D., Pfau, J., and Krueger, D. Goal Misgeneralization in Deep Reinforcement Learning. In *Proceedings of the 39th International Conference on Machine Learning*, pp. 12004–12019. PMLR, June 2022. URL <https://proceedings.mlr.press/v162/langosco22a.html>. ISSN: 2640-3498.
- Leask, P., Bussmann, B., Pearce, M., Bloom, J., Tigges, C., Moubayed, N. A., Sharkey, L., and Nanda, N. Sparse autoencoders do not find canonical units of analysis, 2025. URL <https://arxiv.org/abs/2502.04878>.
- Lieberum, T., Rajamanoharan, S., Conmy, A., Smith, L., Sonnerat, N., Varma, V., Kramár, J., Dragan, A., Shah, R., and Nanda, N. Gemma scope: Open sparse autoencoders everywhere all at once on gemma 2, 2024. URL <https://arxiv.org/abs/2408.05147>.
- Liu, Y., Han, T., Ma, S., Zhang, J., Yang, Y., Tian, J., He, H., Li, A., He, M., Liu, Z., Wu, Z., Zhao, L., Zhu, D., Li, X., Qiang, N., Shen, D., Liu, T., and Ge, B. Summary of chatgpt-related research and perspective towards the future of large language models. *Meta-Radiology*, 1(2): 100017, September 2023. ISSN 2950-1628. doi: 10.1016/j.metrad.2023.100017. URL <http://dx.doi.org/10.1016/j.metrad.2023.100017>.
- Makhzani, A. and Frey, B. k-sparse autoencoders. *arXiv preprint arXiv:1312.5663*, 2013.
- Marks, S., Rager, C., Michaud, E. J., Belinkov, Y., Bau, D., and Mueller, A. Sparse feature circuits: Discovering and editing interpretable causal graphs in language models, 2024.
- Mini, U., Grietzer, P., Sharma, M., Meek, A., MacDiarmid, M., and Turner, A. M. Understanding and Controlling a Maze-Solving Policy Network, 2023. URL <http://arxiv.org/abs/2310.08043>. arXiv:2310.08043 [cs].
- Nanda, N. and Conmy, A. Progress update #1 from the gdm mech interp team: Full update. https://www.alignmentforum.org/posts/C5KAZQib3bzzpeyrg/progress-update-1-from-the-gdm-mech-interp-team-full-update#Activation_Steering_with_SAEs, 2024. Accessed: 2024-06-19.
- Naveed, H., Khan, A. U., Qiu, S., Saqib, M., Anwar, S., Usman, M., Akhtar, N., Barnes, N., and Mian, A. A comprehensive overview of large language models, 2024. URL <https://arxiv.org/abs/2307.06435>.
- Neo, C., Cohen, S. B., and Barez, F. Interpreting context look-ups in transformers: Investigating attention-mlp interactions, 2024. URL <https://arxiv.org/abs/2402.15055>.
- Ngo, R., Chan, L., and Mindermann, S. The Alignment Problem from a Deep Learning Perspective, 2022. URL <http://arxiv.org/abs/2209.00626>. arXiv:2209.00626 [cs].
- Olah, C. and Batson, J. Feature manifold toy model. Transformer Circuits May Update, May 2023. URL <https://transformer-circuits.pub/2023/may-update/index.html#feature-manifolds>.
- Olah, C., Cammarata, N., Schubert, L., Goh, G., Petrov, M., and Carter, S. Zoom in: An introduction to circuits. *Distill*, 2020. doi: 10.23915/distill.00024.001. <https://distill.pub/2020/circuits/zoom-in>.
- Olshausen, B. A. and Field, D. J. Sparse coding with an overcomplete basis set: A strategy employed by v1? *Vision Research*, 37(23):3311–3325, 1997. ISSN 0042-6989. doi: [https://doi.org/10.1016/S0042-6989\(97\)00169-7](https://doi.org/10.1016/S0042-6989(97)00169-7). URL <https://www.sciencedirect.com/science/article/pii/S0042698997001697>.
- O’Neill, C., Ye, C., Iyer, K., and Wu, J. F. Disentangling dense embeddings with sparse autoencoders, 2024. URL <https://arxiv.org/abs/2408.00657>.

-
- Raghu, M., Gilmer, J., Yosinski, J., and Sohl-Dickstein, J. N. Svcca: Singular vector canonical correlation analysis for deep learning dynamics and interpretability. In *Neural Information Processing Systems*, 2017. URL <https://api.semanticscholar.org/CorpusID:23890457>.
- Rajamanoharan, S., Conmy, A., Smith, L., Lieberum, T., Varma, V., Kramár, J., Shah, R., and Nanda, N. Improving dictionary learning with gated sparse autoencoders, 2024a. URL <https://arxiv.org/abs/2404.16014>.
- Rajamanoharan, S., Lieberum, T., Sonnerat, N., Conmy, A., Varma, V., Kramár, J., and Nanda, N. Jumping ahead: Improving reconstruction fidelity with jumprelu sparse autoencoders, 2024b. URL <https://arxiv.org/abs/2407.14435>.
- Rimsky, N., Gabrieli, N., Schulz, J., Tong, M., Hubinger, E., and Turner, A. M. Steering llama 2 via contrastive activation addition, 2024.
- Schubert, L., Voss, C., Cammarata, N., Goh, G., and Olah, C. High-low frequency detectors. *Distill*, 2021. doi: 10.23915/distill.00024.005. <https://distill.pub/2020/circuits/frequency-edges>.
- Shah, R., Varma, V., Kumar, R., Phuong, M., Krakovna, V., Uesato, J., and Kenton, Z. Goal Misgeneralization: Why Correct Specifications Aren’t Enough For Correct Goals, November 2022. URL <http://arxiv.org/abs/2210.01790>. arXiv:2210.01790 [cs].
- Sharkey, L., Braun, D., and Millidge, B. Interim research report: Taking features out of superposition with sparse autoencoders. *AI Alignment Forum*, 2022. URL <https://www.alignmentforum.org/posts/z6QQJbtpkEAX3Aojj/interim-research-report-taking-features-out-of-superposition>.
- Sharkey, L., Bushnaq, L., Braun, D., Hex, S., and Goldowsky-Dill, N. A list of 45 mech interp project ideas from apollo research. <https://www.lesswrong.com/posts/KfkpgXdgRheSRWdy8/a-list-of-45-mech-interp-project-ideas-from-apollo-research>, 2024. Accessed: 2024-07-25.
- Sharma, M., Tong, M., Korbak, T., Duvenaud, D., Askill, A., Bowman, S. R., Cheng, N., Durmus, E., Hatfield-Dodds, Z., Johnston, S. R., Kravec, S., Maxwell, T., McCandlish, S., Ndousse, K., Rausch, O., Schiefer, N., Yan, D., Zhang, M., and Perez, E. Towards Understanding Sycophancy in Language Models, October 2023. URL <http://arxiv.org/abs/2310.13548>. arXiv:2310.13548 [cs, stat].
- Sucholutsky, I., Muttenthaler, L., Weller, A., Peng, A., Bobu, A., Kim, B., Love, B. C., Grant, E., Achterberg, J., Tenenbaum, J. B., Collins, K. M., Hermann, K. L., Oktar, K., Greff, K., Hebart, M. N., Jacoby, N., Zhang, Q., Marjeh, R., Geirhos, R., Chen, S., Kornblith, S., Rane, S., Konkle, T., O’Connell, T. P., Unterthiner, T., Lampinen, A. K., Müller, K.-R., Toneva, M., and Griffiths, T. L. Getting aligned on representational alignment. *CoRR*, abs/2310.13018, 2023.
- Team, G., Mesnard, T., Hardin, C., Dadashi, R., Bhupatiraju, S., Pathak, S., Sifre, L., Rivière, M., Kale, M. S., Love, J., Tafti, P., Hussenot, L., Sessa, P. G., Chowdhery, A., Roberts, A., Barua, A., Botev, A., Castro-Ros, A., Slone, A., Héliou, A., Tacchetti, A., Bulanova, A., Paterson, A., Tsai, B., Shahriari, B., Lan, C. L., Choquette-Choo, C. A., Crepy, C., Cer, D., Ippolito, D., Reid, D., Buchatskaya, E., Ni, E., Noland, E., Yan, G., Tucker, G., Muraru, G.-C., Rozhdestvenskiy, G., Michalewski, H., Tenney, I., Grishchenko, I., Austin, J., Keeling, J., Labanowski, J., Lespiau, J.-B., Stanway, J., Brennan, J., Chen, J., Ferret, J., Chiu, J., Mao-Jones, J., Lee, K., Yu, K., Millican, K., Sjoesund, L. L., Lee, L., Dixon, L., Reid, M., Mikula, M., Wirth, M., Sharman, M., Chinaev, N., Thain, N., Bachem, O., Chang, O., Wahltinez, O., Bailey, P., Michel, P., Yotov, P., Chaabouni, R., Comanescu, R., Jana, R., Anil, R., McIlroy, R., Liu, R., Mullins, R., Smith, S. L., Borgeaud, S., Girgin, S., Douglas, S., Pandya, S., Shakeri, S., De, S., Klimenko, T., Hennigan, T., Feinberg, V., Stokowiec, W., hui Chen, Y., Ahmed, Z., Gong, Z., Warkentin, T., Peran, L., Giang, M., Farabet, C., Vinyals, O., Dean, J., Kavukcuoglu, K., Hassabis, D., Ghahramani, Z., Eck, D., Barral, J., Pereira, F., Collins, E., Joulis, A., Fiedel, N., Senter, E., Andreev, A., and Kenealy, K. Gemma: Open models based on gemini research and technology, 2024a. URL <https://arxiv.org/abs/2403.08295>.

-
- Team, G., Riviere, M., Pathak, S., Sessa, P. G., Hardin, C., Bhupatiraju, S., Hussenot, L., Mesnard, T., Shahriari, B., Ramé, A., Ferret, J., Liu, P., Tafti, P., Friesen, A., Casbon, M., Ramos, S., Kumar, R., Lan, C. L., Jerome, S., Tsitsulin, A., Vieillard, N., Stanczyk, P., Girgin, S., Momchev, N., Hoffman, M., Thakoor, S., Grill, J.-B., Neyshabur, B., Bachem, O., Walton, A., Severyn, A., Parrish, A., Ahmad, A., Hutchison, A., Abdagic, A., Carl, A., Shen, A., Brock, A., Coenen, A., Laforge, A., Paterson, A., Bastian, B., Piot, B., Wu, B., Royal, B., Chen, C., Kumar, C., Perry, C., Welty, C., Choquette-Choo, C. A., Sinopalnikov, D., Weinberger, D., Vijaykumar, D., Rogozińska, D., Herbison, D., Bandy, E., Wang, E., Noland, E., Moreira, E., Senter, E., Eltyshev, E., Visin, F., Rasskin, G., Wei, G., Cameron, G., Martins, G., Hashemi, H., Klimczak-Plucińska, H., Batra, H., Dhand, H., Nardini, I., Mein, J., Zhou, J., Svensson, J., Stanway, J., Chan, J., Zhou, J. P., Carrasqueira, J., Iljazi, J., Becker, J., Fernandez, J., van Amersfoort, J., Gordon, J., Lipschultz, J., Newlan, J., yeong Ji, J., Mohamed, K., Badola, K., Black, K., Millican, K., McDonell, K., Nguyen, K., Sodhia, K., Greene, K., Sjoesund, L. L., Usui, L., Sifre, L., Heuermann, L., Lago, L., McNealus, L., Soares, L. B., Kilpatrick, L., Dixon, L., Martins, L., Reid, M., Singh, M., Iverson, M., Görner, M., Velloso, M., Wirth, M., Davidow, M., Miller, M., Rahtz, M., Watson, M., Risdal, M., Kazemi, M., Moynihan, M., Zhang, M., Kahng, M., Park, M., Rahman, M., Khatwani, M., Dao, N., Bardoliwalla, N., Devanathan, N., Dumai, N., Chauhan, N., Wahltinez, O., Botarda, P., Barnes, P., Barham, P., Michel, P., Jin, P., Georgiev, P., Culliton, P., Kuppala, P., Comanescu, R., Berhej, R., Jana, R., Rokni, R. A., Agarwal, R., Mullins, R., Saadat, S., Carthy, S. M., Perrin, S., Arnold, S. M. R., Krause, S., Dai, S., Garg, S., Sheth, S., Ronstrom, S., Chan, S., Jordan, T., Yu, T., Eccles, T., Hennigan, T., Kocisky, T., Doshi, T., Jain, V., Yadav, V., Meshram, V., Dharmadhikari, V., Barkley, W., Wei, W., Ye, W., Han, W., Kwon, W., Xu, X., Shen, Z., Gong, Z., Wei, Z., Cotruta, V., Kirk, P., Rao, A., Giang, M., Peran, L., Warkentin, T., Collins, E., Barral, J., Ghahramani, Z., Hadsell, R., Sculley, D., Banks, J., Dragan, A., Petrov, S., Vinyals, O., Dean, J., Hassabis, D., Kavukcuoglu, K., Farabet, C., Buchatskaya, E., Borgeaud, S., Fiedel, N., Joulin, A., Kenealy, K., Dadashi, R., and Andreev, A. Gemma 2: Improving open language models at a practical size, 2024b. URL <https://arxiv.org/abs/2408.00118>.
- team, L., Barrault, L., Duquenne, P.-A., Elbayad, M., Kozhevnikov, A., Alastruey, B., Andrews, P., Coria, M., Couairon, G., Costa-jussà, M. R., Dale, D., Elsahar, H., Heffernan, K., Janeiro, J. M., Tran, T., Ropers, C., Sánchez, E., Roman, R. S., Mourachko, A., Saleem, S., and Schwenk, H. Large concept models: Language modeling in a sentence representation space, 2024. URL <https://arxiv.org/abs/2412.08821>.
- Templeton, A., Conerly, T., Marcus, J., Lindsey, J., Bricken, T., Chen, B., Pearce, A., Citro, C., Ameisen, E., Jones, A., Cunningham, H., Turner, N. L., McDougall, C., MacDiarmid, M., Freeman, C. D., Sumers, T. R., Rees, E., Batson, J., Jermyn, A., Carter, S., Olah, C., and Henighan, T. Scaling monosemanticity: Extracting interpretable features from claude 3 sonnet. *Transformer Circuits Thread*, 2024. URL <https://transformer-circuits.pub/2024/scaling-monosemanticity/index.html>.
- Thasarathan, H., Forsyth, J., Fel, T., Kowal, M., and Derpanis, K. Universal sparse autoencoders: Interpretable cross-model concept alignment, 2025. URL <https://arxiv.org/abs/2502.03714>.
- Till, D. Do sparse autoencoders find 'true features'?, 2023. URL <https://www.lesswrong.com/posts/QoR8noAB3Mp2KBA4B/do-sparse-autoencoders-find-true-features>. Accessed: 2025-01-29.
- Turner, A. M., Thiergart, L., Udell, D., Leech, G., Mini, U., and MacDiarmid, M. Activation addition: Steering language models without optimization, 2023.
- Vaswani, A., Shazeer, N., Parmar, N., Uszkoreit, J., Jones, L., Gomez, A. N., Kaiser, Ł., and Polosukhin, I. Attention is all you need. *Advances in neural information processing systems*, 30, 2017.
- Wang, L., Hu, L., Gu, J., Wu, Y., Hu, Z., He, K., and Hopcroft, J. Towards understanding learning representations: To what extent do different neural networks learn the same representation. In *Advances in Neural Information Processing Systems*, volume 31, 2018a. URL <https://proceedings.neurips.cc/paper/2018/file/5fc34ed307aac159a30d81181c99847e-Paper.pdf>.

-
- Wang, L., Hu, L., Gu, J., Wu, Y., Hu, Z., He, K., and Hopcroft, J. Towards understanding learning representations: To what extent do different neural networks learn the same representation. In *Proceedings of the 32nd International Conference on Neural Information Processing Systems, NIPS'18*, pp. 9607–9616, Red Hook, NY, USA, 2018b. Curran Associates Inc. ISBN 9781510860964.
- Weber, M., Fu, D., Anthony, Q., Oren, Y., Adams, S., Alexandrov, A., Lyu, X., Nguyen, H., Yao, X., Adams, V., Athiwaratkun, B., Chalamala, R., Chen, K., Ryabinin, M., Dao, T., Liang, P., Ré, C., Rish, I., and Zhang, C. Redpajama: an open dataset for training large language models, 2024. URL <https://arxiv.org/abs/2411.12372>.
- Yosinski, J., Clune, J., Bengio, Y., and Lipson, H. How transferable are features in deep neural networks? In *Proceedings of the 27th International Conference on Neural Information Processing Systems - Volume 2, NIPS'14*, pp. 3320–3328, Cambridge, MA, USA, 2014. MIT Press.
- Zou, A., Phan, L., Chen, S., Campbell, J., Guo, P., Ren, R., Pan, A., Yin, X., Mazeika, M., Dombrowski, A.-K., Goel, S., Li, N., Byun, M. J., Wang, Z., Mallen, A., Basart, S., Koyejo, S., Song, D., Fredrikson, M., Kolter, J. Z., and Hendrycks, D. Representation engineering: A top-down approach to ai transparency, 2023.

A LIST OF MODELS ANALYZED IN EXPERIMENTS

1. Pythia-70m VS Pythia-160m
2. Gemma-1-2B VS Gemma-2-2B
3. Gemma-2-2B vs Gemma-2-9B
4. Gemma-2-9B vs Gemma-2-9B-Instruct
5. Gemma-1-2B vs Gemma-1-2B-Instruct (at Layer 12)
6. Llama 3-8B and Llama 3.1-8B (at Layer 25)
7. Pythia-70m vs Randomized Pythia-70m (*Baseline Comparisons*)
8. TinyStories-1L-21M (*Within Model Comparisons*)

Unless otherwise specified, all experiments filter feature pairs by non-concept keywords, 1-1, and low correlation (less than 0.1).

B TRAINED SAE METRIC EVALUATIONS

For SAEs with an expansion factor of 64 (and thus 32768 total latents) and a top-k of 32 trained on residual stream layers of Pythia-70m using 100 million tokens from the RedPajama dataset, we obtain explained variances of between 0.70 to 0.82 ($\mu = 0.75, \sigma = 0.04$), cosine similarities between 0.92 to 0.99, cross entropy losses between 0.78 to 0.94, and L1 norm between 24.0 to 50.75 ($\mu = 35.55, \sigma = 8.78$). Likewise, these are also SAEs with good reconstruction and sparsity metrics.

In general, all of our custom trained SAEs on Pythia-70m and on Pythia-160m have similar metrics as the ones reported for the SAEs in this section. We evaluate the SAEs on SAEBench (Karvonen et al., 2024).

For the random SAEs trained on identical conditions as the non-random SAEs mentioned above, but on a randomized Pythia-70m with the embedding layer not being randomized, we obtain explained variances of between 0.63 to 0.80 ($\mu = 0.71, \sigma = 0.006$), cosine similarities 1, cross entropy losses of 1, and L1 norm between 27.38 to 38.25. These results are similar to the results for Pythia-70m-deduped SAEs found by Heap et al. (2025), and indicates SAEs with good reconstruction and sparsity metrics.

However, for our experiments that use these custom trained SAEs, we find that only around 2 to 4% of feature pairs are kept on average, in contrast to the 20 to 30% of features kept when running the pretrained models hosted by Eleuther and SAELens. We attribute this low amount of feature spaces to the quality of our trained SAEs in capturing features; while SAEs like those trained by Eleuther used around 8 billion tokens, our SAEs were trained using 100 million tokens, and as such may not be capturing features as well.

C RESULTS FROM MORE MODELS

C.1 GEMMA-2-2B VS GEMMA-2-9B RESULTS

We compare Gemma-2-2B vs Gemma-2-9B at several layers of each model, which each have 25 and 41 layers, respectively. Each SAE has a width of 16384 features and uses JumpReLU (Rajamanoharan et al., 2024b), and is hosted on SAELens. We obtain activations from OpenWebText using 150 samples with a max sequence length of 150, for a total of 22.5k tokens. Figure 4 shows SVCCA and RSA scores after filtering keywords and for 1-1. On average, around 20% of feature pairs are kept after filtering. In particular, the L11 vs L21 comparison achieves an SVCCA score of 0.70 (while mean random pairing has a score of 0.009) and an RSA score of 0.195 (while mean random pairing has a score of 4.38×10^{-4}).

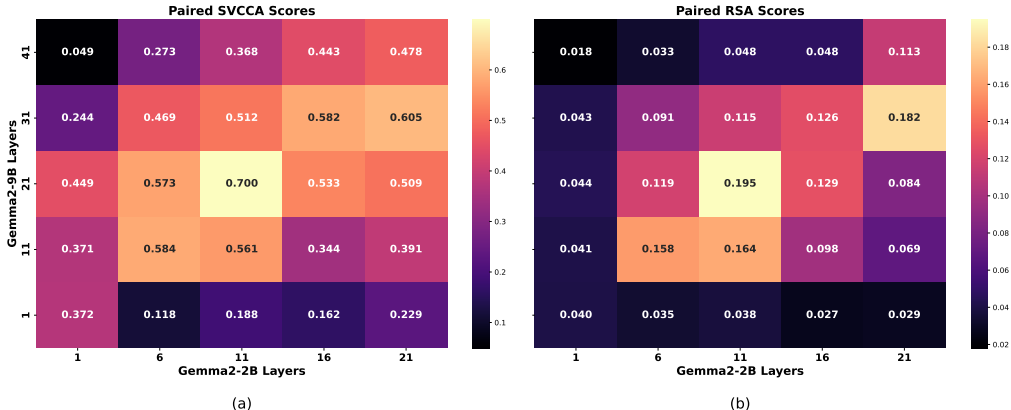


Figure 4: (a) SVCCA and (b) RSA 1-1 paired scores of SAEs for layers in Gemma-2-2B vs layers in Gemma-2-9B. Middle layers have the best performance. We exclude layers 0, as we observe they always have non-statistically significant similarity.

C.2 BASE VS FINE TUNED RESULTS

We compare Gemma-2-2B vs Gemma-2-9B-Instruct, a fine tuned version, at Layers 9, 20, and 31 of each model. Each SAE has a width of 16384 features. Only the pretrained SAEs for layers 9, 20 and 31 were publically available online and hosted on SAELens. We obtain activations from the RedPajamas dataset (Weber et al., 2024) using 150 samples with a max sequence length of 150, for a total of 22.5k tokens. On average, 22.2% of feature pairs are kept after filtering, with the range between 16.4% and 33.5%. Figure 5 shows that closer layers had higher SVCCA scores, while RSA scores were low except for matching layers. This is consistent with previous work which found that SAE features can transfer across base to fine-tuned language models (Kissane et al., 2024a; Kutsyk et al., 2024).

We also compare Gemma-1-2B vs Gemma-1-2B-Instruct, a fine tuned version, at Layer 12 of each model. Each SAE has a width of 16384 features. We obtain activations using 150 samples with a max sequence length of 150, for a total of 22.5k tokens. After filtering, the comparison achieves an SVCCA score of 0.84 (while mean random pairing has a score of 0.008) and an RSA score of 0.25 (while mean random pairing has a score of 4.29×10^{-4}). Around 50% of feature pairs are kept after filtering.

C.3 LLAMA 3 RESULTS

We compare Llama 3-8B-Instruct and Llama 3.1-8B at each model’s Layer 25 residual stream, a later layer in both models. The Llama 3 SAE has a width of 65536 features and uses Gated ReLU (Rajamanoharan et al., 2024a), while the Llama 3.1 SAE has a width of 32768 features and uses JumpReLU (Rajamanoharan et al., 2024b). We obtain activations using 100 samples with a max

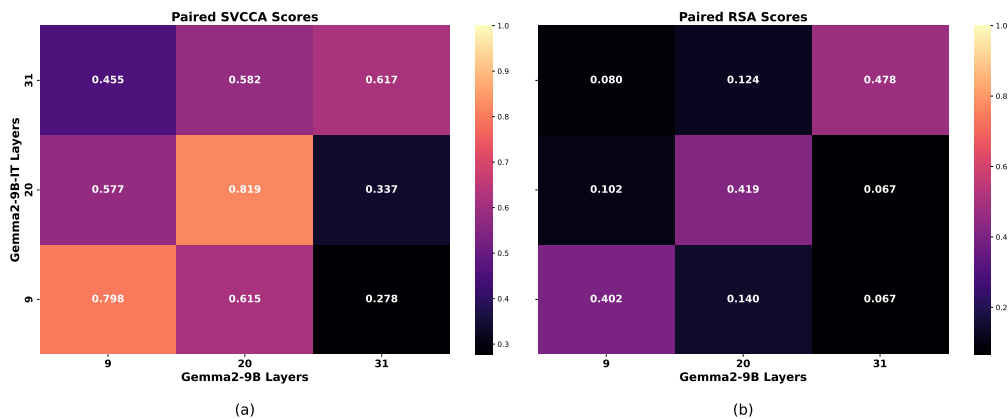


Figure 5: Gemma-2-9B vs Gemma-2-9B-Instruct 1-1 paired SAE scores for (a) SVCCA and (b) RSA.

sequence length of 100, for a total of 10000 tokens. After filtering, this comparison achieves an SVCCA score of 0.3, comparable to the score of later layers in both Gemma and Pythia.

D BASELINE COMPARISONS TO SAEs TRAINED ON LLMs WITH RANDOMIZED WEIGHTS

Recent research has demonstrated that training SAEs on randomly initialized transformers—where parameters are independently sampled from a Gaussian distribution rather than learned from text data—yields latent representations that are similarly interpretable to those from trained transformers (Heap et al., 2025). One caveat is that the interpretable features of SAEs trained on "randomized" LLMs tend to activate on simple features, such as ones that activate on specific single tokens instead of more general concepts, rather than complex abstract features learned by middle to later layer SAEs. The authors propose that there may be cases where "simple" interpretable latents may arise from the inherent sparsity of the text data used to train language models, rather than from uncovering the computational structure embedded within the underlying model. Thus, we test whether the feature similarities found across LLMs are due to the sparsity of the training data or due to the computational structure. We run experiments comparing the representational similarity of SAE features trained on randomized LLMs to SAE trained on the original LLMs. We call the former "random SAEs", and the latter "non-random SAEs".

We find that, relative to other across model experiments, there is little similarity between the non-random SAEs and random SAEs, which suggests that our method is demonstrating SAE feature space similarity that is capturing the model’s computational structure, and is not just capturing similarity due to interpretability from the inherent sparsity of the text data. In particular, not even the same layers have medium similarity. However, the small amounts of similarity do suggest that SAEs trained on even randomized LLMs can capture features in the data, which is consistent with the interpretable "simple, low information" features, such as those that just activate on single tokens, that were also present in random SAEs found by Heap et al. (2025).

SAE Models. For Pythia-70m, we compare residual stream layer SAEs trained a randomized Pythia-70m, to SAEs trained on the original Pythia-70m. Both SAEs were trained using 100 million tokens from the RedPajama dataset (Weber et al., 2024), with an expansion factor of 64 and a Top-K of 32. The embedding layer was not randomized. We evaluate the SAEs on SAEbench (Karvonen et al., 2024) and report their results in Section §B. Overall, all SAEs obtained good reconstruction and sparsity metric scores.

Results. As shown in Figure 6, using 200 samples with a max sequence length of 200 for a total of 40k tokens, we find that after filtering, we obtain very low SVCCA and RSA scores, indicating that random SAEs do not find features with notably similar relations compared to non-random SAEs. In comparison, the non-random SAEs obtained higher similarity scores when compared to other SAEs

also trained on Pythia-70m, such as when comparing to the Eleuther SAEs as shown in Figure 12. Additionally, we find that only 1% of feature pairs are kept on average. The reason why this may occur is discussed in Section §B.

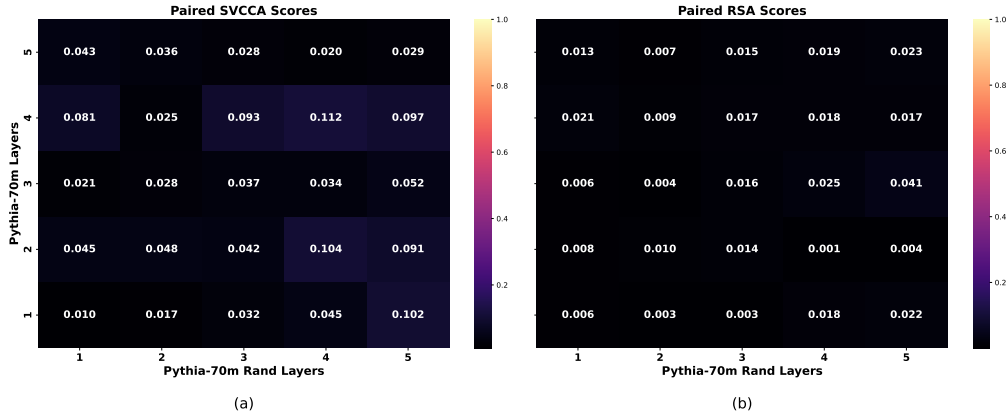


Figure 6: Baseline Comparisons with SAEs trained on Randomized Pythia-70m: (a) SVCCA 1-1 paired scores of SAEs, (b) RSA 1-1 paired scores of SAEs.

E WITHIN MODEL FEATURE SPACE SIMILARITY RESULTS

E.1 COMPARING THE SAME SAE TO THEMSELVES

As a sanity check that our method works, we compare running the same Pythia SAEs against themselves using our method. As expected, the same layers achieve 99 to 100% similar activation correlation, SVCCA, and RSA scores. However, for other layer pairs, our results obtained for the same model demonstrate that similarity scores greatly depend on the quality of the SAE that is trained. As shown in Figure 7, the Pythia-70m 32k latent SAEs trained on 8.2 billion tokens from The Pile show notable similarity between middle and later layers. However, as shown in Figure 8, the Pythia-70m 32k latent SAEs trained on only 100 million tokens from RedPajamas, which were trained on 1% of the training data as Eleuther’s SAEs, show almost no similarity for some middle / later layer pairs. This demonstrates that while models may have notable similarity, these similarities may not always be revealed by just any SAE; the quality of the SAE in capturing these features is important. Additionally, different SAEs may reveal different features. For instance, the Layer 5 to Layer 1 pair in Figure 7 shows low similarity, while the same pair in Figure 8 shows medium-high similarity.

This is consistent with recent results which found that SAEs do not learn consistent features (Leask et al., 2025; Hindupur et al., 2025). Thus, while we show that certain subspaces learned by LLMs have high similarity, as revealed by SAEs, these subspaces may not always be consistently captured by arbitrary SAEs. This demonstrates a limitation by SAEs- they can capture different features that are shared across models, but cannot do this consistently. Thus, future work can attempt to address this limitation to develop SAEs that capture features more consistently. Indeed, recent work has already developed "universal SAEs" that can better capture features found across models (Thasarathan et al., 2025).

E.2 COMPARING SAEs TRAINED WITH DIFFERENT SEEDS

Pythia-70m Results . We trained two SAEs with different seeds on Pythia-70m. As discussed in Section §E.1, due to training limitations such as only using 100 million tokens during training, these SAEs do not capture features as well as higher quality SAEs such as Eleuther’s SAEs trained on 8.2 billion tokens from the Pile. Thus, we compare the results of SAEs trained on different seeds with the results of Figure 8, which compare the SAE with itself as a baseline, rather than assuming that the adjacent layers must be highly similar (or in other words, Figure 7 would not be suitable as a baseline).

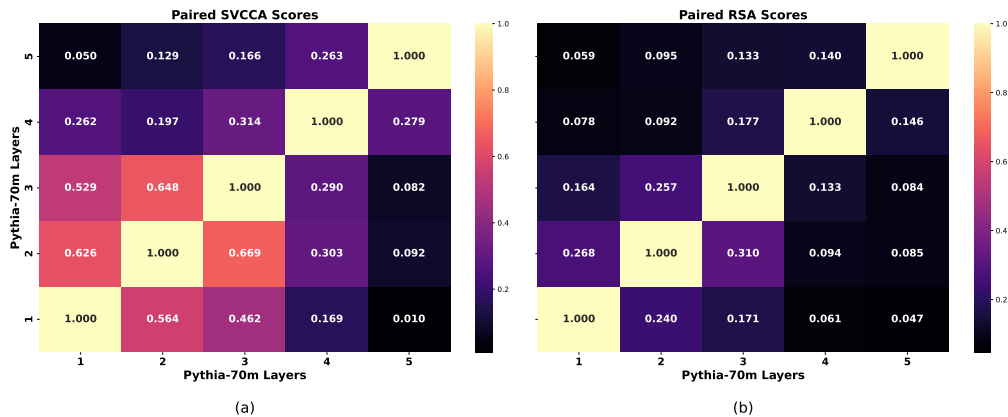


Figure 7: (a) SVCCA 1-1 paired scores of the same SAE trained on 8.2 billion tokens from The Pile by Eleuther, (b) RSA 1-1 paired scores of the same SAE.

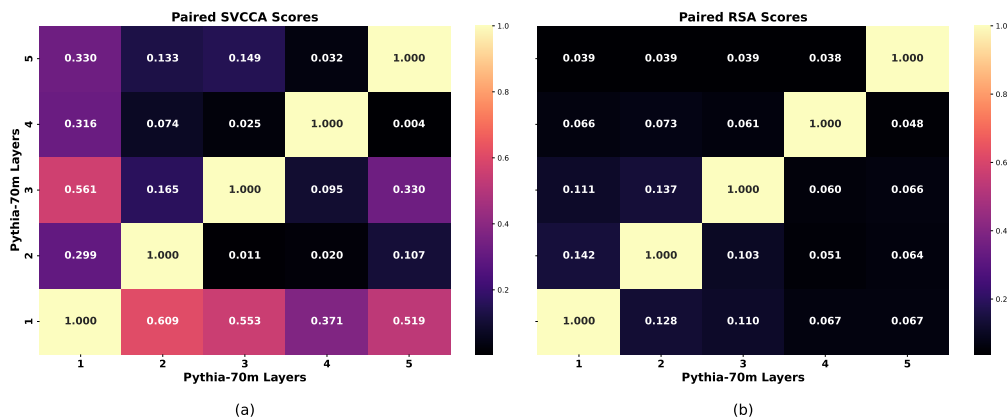


Figure 8: (a) SVCCA 1-1 paired scores of the same SAE trained on 100 million tokens from RedPajamas, (b) RSA 1-1 paired scores of the same SAE.

The SAE results on different seeds is shown in Figure 9, and show some resemblance to the results of Figure 8. Notably, this occurs in how the first layer (bottom row) have high similarities, while the later layer comparisons show very low or no similarity. However, there are still notable dissimilarities; for instance, the same-layer comparisons along the diagonal for SAEs trained on different seeds only have a similarity of 0.376 on average, which is much less than the similarity of 1 for the same SAEs. Thus, the results of comparing SAEs trained on different seeds are similar to the results of comparing the same SAE to itself, but with notable differences.

As mentioned before in Section §E.1, this is consistent with recent results which found that SAEs do not learn consistent features (Leask et al., 2025; Hindupur et al., 2025). Despite not finding the same features, which can be viewed as a form of strong universality, these SAEs still show notable similarity. This can be viewed as a form of weak universality; see Appendix H for further discussion on this topic.

Tinystories Results . To examine SAE feature space similarities when trained on the same model, we train multiple SAEs on a one-layer Tinystories model.

SAE Training Parameters. We train two SAEs at different seeds for a TinyStories-1L-21M model (Eldan, 2023). Both SAEs are trained at 30k steps with expansion factor of 16, for a 16384 total features, on a TinyStories dataset, and using ReLU as the activation function. We use a batch size of 4096 tokens and train with an Adam optimizer, applying a constant learning rate of 1×10^{-5} . The learning rate follows a warm-up-free schedule with a decay period spanning 20% of the total

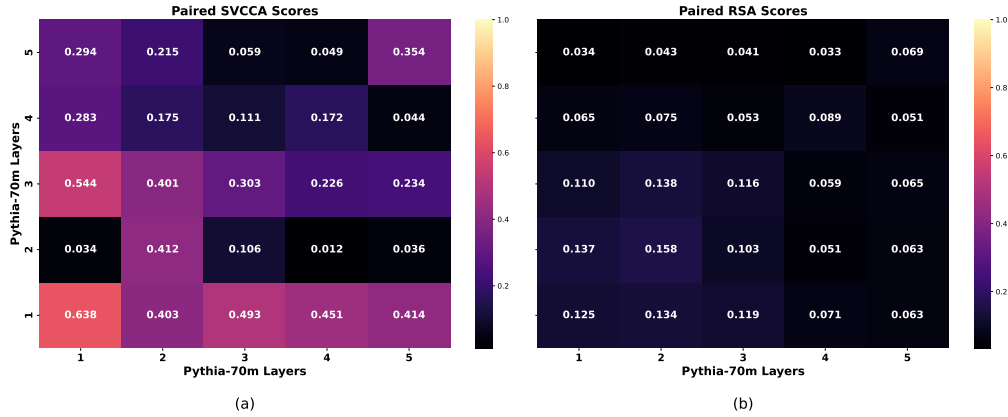


Figure 9: (a) SVCCA 1-1 paired scores of two SAEs trained with different seeds on 100 million tokens from RedPajamas, (b) RSA 1-1 paired scores of the SAEs. The SAE on the rows (y-axis) is the same SAE as the one in Figure 8.

training steps. L1 sparsity regularization is applied with a coefficient of 5, and its effect gradually increases over the first 5% of training steps. We obtain SAE activations using 500 samples from the TinyStories dataset with a max sequence length of 128 (for a total of 64000 tokens).

ManyA-to-1B. This experiment allows multiple features from SAE *A* to map onto a single feature from SAE *B*. Before filtering non-concept features, this comparison achieves an SVCCA score of 0.73, retaining 9930 feature pairs. After filtering for non-concept features (for this study, we only filter for periods and padding tokens), this pair achieves an SVCCA score of 0.94. Randomly paired achieves a score of 0.004 for 10 runs. We found that filtering for 1-1 did not change the score much. In contrast, for 10 random runs where we randomly choose 7 tokens that are not part of the non-concept tokens, the filtering of these randomly chosen tokens does not change the unfiltered SVCCA score of 0.73.

1A-to-ManyB. This experiment allows multiple features from SAE *B* to map onto a single feature from SAE *A*. Before filtering nonconcept features, this comparison achieves an SVCCA score of 0.8. After filtering for nonconcept features, this pair achieves an SVCCA score of 0.94, retaining 13073 feature pairs. We found that filtering for 1-1 did not change the score much. The results for "randomly chosen tokens filtering" and "randomly shuffled pairing" match those for the ManyA-to-1B experiment.

Cosine Similarity. Given that these SAEs were trained on the same model, we also compare use cosine similarity instead of activation correlation to pair the features. We obtain an average cosine similarity of 0.9. When using cosine similarity to pair the SAE features, we obtain an SVCCA score of 0.92. This occurs whether we use 1A-to-ManyB or ManyA-to-1B. Every feature finds a unique pairing, despite neither matrix containing exact matches for their features with one another.

Different SAE Widths. We find similar results for SAEs trained using an expansion factor of 8, for 8192 total features. For ManyA-to-1B, before filtering, an SVCCA score of 0.84 is achieved, and after filtering, an SVCCA score of 0.94 is achieved. For 1A-to-ManyB, before filtering, an SVCCA score of 0.87 is achieved, and after filtering, an SVCCA score of 0.94 is achieved.

E.3 COMPARING SAEs WITH DIFFERENT WIDTHS

Figure 10 shows SAEs with 32k latents vs SAEs with 16k latents, both trained on Pythia-70m. This 32k SAE is the SAE shown on the columns (x-axis) of Figure 9. After filtering, around 3.47% of feature pairs are kept on average. Figure 11 shows an SAE with 64k latents vs an SAE with 32k latents, both trained on Pythia-70m. After filtering, around 3.88% of feature pairs are kept on average. The reason why this may occur is discussed in Section §B.

In general, we do not find noticeable trends in scores as we vary SAE widths. This may be because each SAE varies in the features they capture Leask et al. (2025), so while they capture feature

similarities across models, the similar features that they do capture are not the same for each SAE. We did not evaluate for feature splitting or absorption (Chanin et al., 2024).

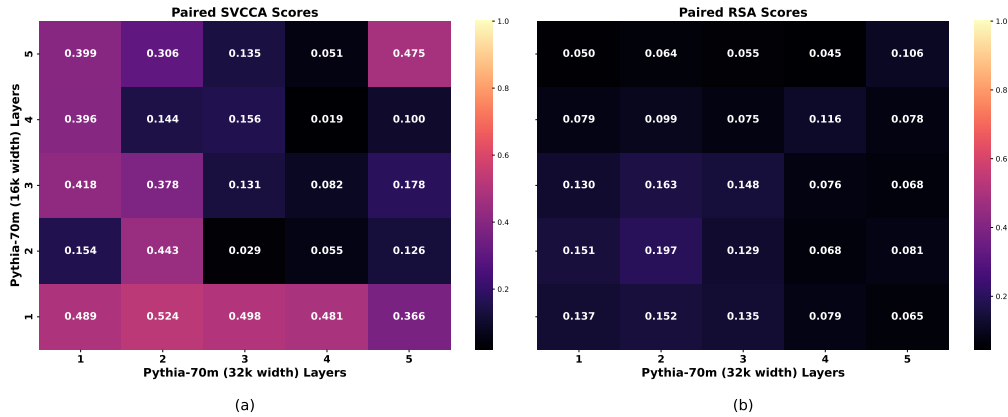


Figure 10: (a) SVCCA 1-1 paired scores of an SAE with 32k latents vs an SAE with 16k latents, (b) RSA 1-1 paired scores of the SAEs.

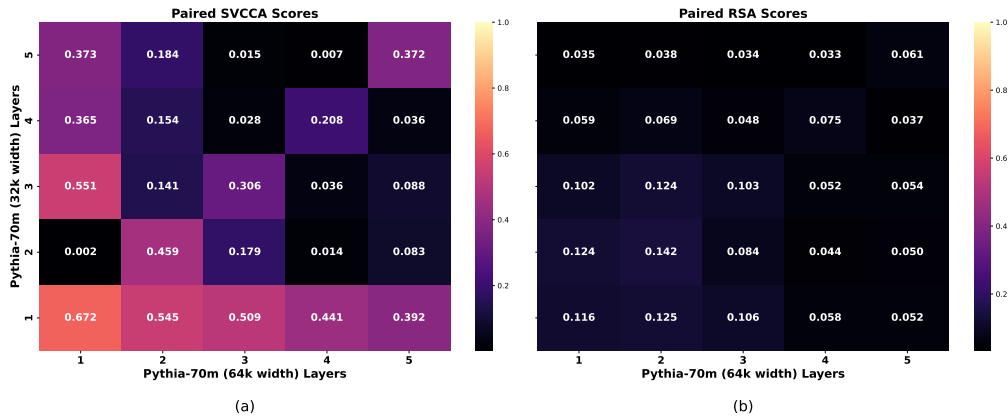


Figure 11: (a) SVCCA 1-1 paired scores of an SAE with 64k latents vs an SAE with 32k latents, (b) RSA 1-1 paired scores of the SAEs.

E.4 COMPARING SAEs TRAINED ON DIFFERENT DATASETS

We compare SAEs on Pythia-70m trained on different training data. We trained an SAE trained on the residual stream layers of Pythia-70m using 100 million tokens using the RedPajama dataset at a context length of 256, with 32768 feature neurons (an expansion factor of 64 and Top-K) of 32. We compare our SAE with Eleuther’s SAE trained at residual streams using 8.2 billion tokens from the Pile training set at a context length of 2049 with 32768 feature neurons and Top-K of 16.

To obtain activations, we use 200 samples with a max sequence length of 200, and after filtering around 4.58% of feature pairs are kept on average, in contrast to the 20 to 30% of feature pairs kept by comparing Eleuther’s pretrained SAEs with each other, perhaps due to the lower quality of our SAEs as discussed in Section §B.

Figure 12 shows that the two sets of SAEs show some similarities, such as at Layers 1, 3, and 5, but also notable dissimilarities, such as having nearly no similarities at Layers 2 and 4. These discrepancies may be due to the difference in training data, as it has been shown that SAEs are highly dataset dependent (Kissane et al., 2024b). However, despite these discrepancies in individual features, the feature subspaces we compare appears to be highly similar, which may suggest that while the

specific values captured by feature weight vectors may differ, these values lie in similar latent space regions that capture similar semantics.

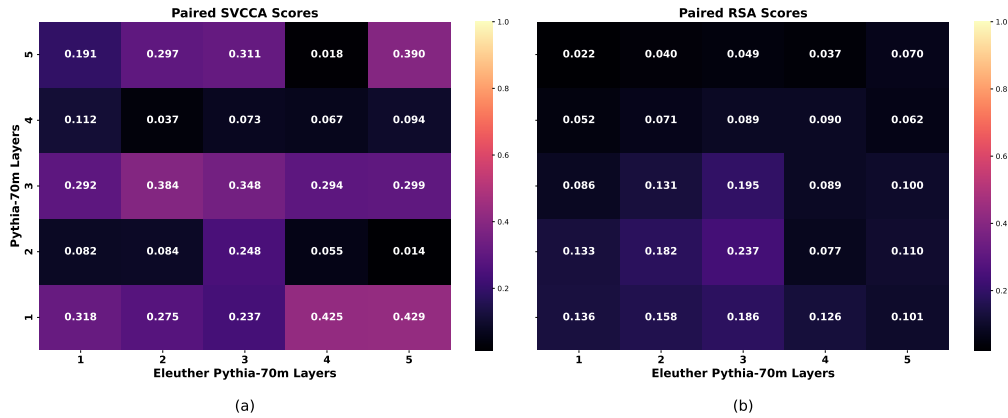


Figure 12: (a) SVCCA 1-1 paired scores of Eleuther’s SAE (trained on 8.2 billion tokens from the Pile) vs our SAE (trained on 100 million tokens from RedPajamas). Both have 32k latents. (b) RSA 1-1 paired scores of the SAEs.

We also train SAEs using 100 million tokens from OpenWebText and compare them to the SAEs we trained on RedPajamas. These results are shown in Figure 13. Similar to the results in Figure 12, we find both similarities and dissimilarities which suggest that SAEs are highly dataset dependent.

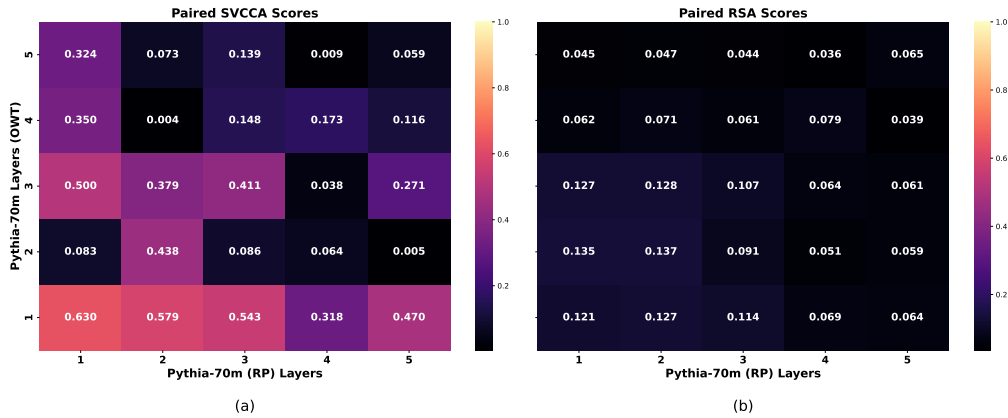


Figure 13: (a) SVCCA 1-1 paired scores of our SAEs trained on RedPajamas (columns, x-axis) vs our SAEs trained on OpenWebText (rows, y-axis). Both have 32k latents. (b) RSA 1-1 paired scores of the SAEs.

F CROSS MODEL SAE WIDTH VARIATION RESULTS

We compare what happens to similarity scores as we increase SAE widths for both Pythia-70m and Pythia-160m. All SAEs were trained using 100 million tokens from RedPajamas and use Top-K of 32. Similar to Section §E.3, we do not find noticeable trends in scores as we vary SAE widths. This may be because each SAE varies in the features they capture, so while they capture feature similarities across models, the similar features that they do capture are not the same for each SAE.

Figure 14 SVCCA and RSA 1-1 paired scores of 24k latent SAEs trained on Pythia-160m vs 16k latent SAEs trained on Pythia-70m, and Figure 15 SVCCA and RSA 1-1 paired scores of 49k latent SAEs trained on Pythia-160m vs 32k latent SAEs trained on Pythia-70m. In both figures, while SVCCA scores are moderately high for some layers, the RSA scores are very low.

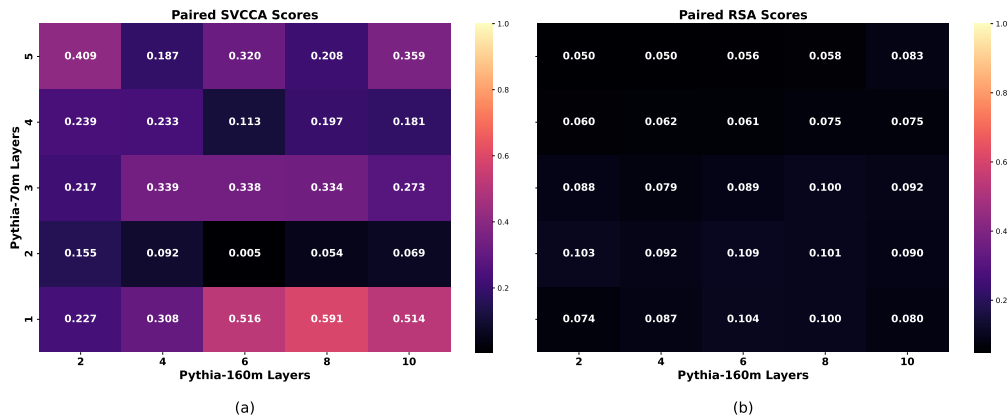


Figure 14: (a) SVCCA 1-1 paired scores of 24k latent SAEs trained on Pythia-160m vs 16k latent SAEs trained on Pythia-70m. (b) RSA 1-1 paired scores of the SAEs.

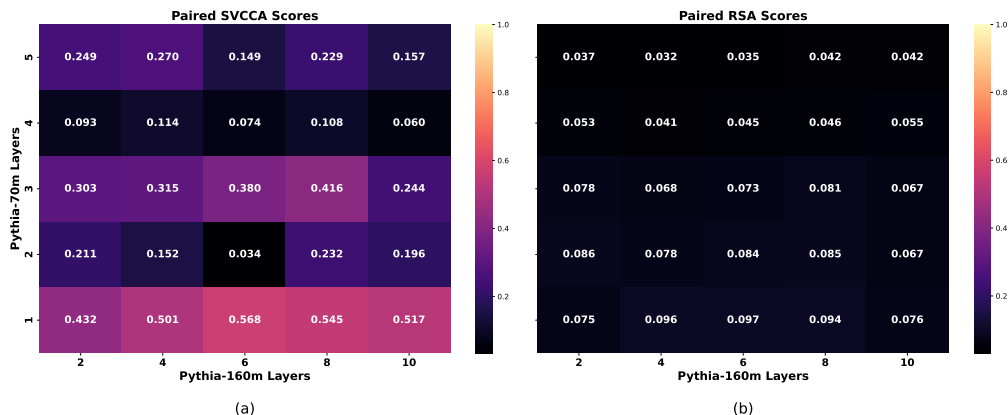


Figure 15: (a) SVCCA 1-1 paired scores of 49k latent SAEs trained on Pythia-160m vs 32k latent SAEs trained on Pythia-70m. (b) RSA 1-1 paired scores of the SAEs.

G VARYING FACTORS USED TO OBTAIN ACTIVATIONS

G.1 COMPARING DIFFERENT DATASETS TO OBTAIN ACTIVATIONS

We compare results using different datasets, namely the RedPajamas and OpenWebText datasets, to obtain dataset activations used for matching features by activation correlation. For Eleuther’s 32k SAEs trained on Pythia-160m vs on Pythia-70m, Figure 16 displays results from using the RedPajamas dataset, whereas Figure 17 displays results from using the OpenWebText dataset. Overall, the results are similar, with scores from OpenWebText being slightly higher in most cases. This demonstrates that our method is not highly dataset dependent when obtaining activations to pair features by correlation.

Note that these results differ from previous results in Figure 2 because for features matching using Many-to-1 (before filtering), we are using Pythia 160m as the model whose features can have "Many" mappings and Pythia 70m as model whose features can only have "1" mapping, whereas the results in Figure 2 reverse these roles. As implied in Section §J, the results of using a model in the "Many" or "1" places of Many-to-1 are not symmetric, partly due to using max correlation to choose a feature’s partner.

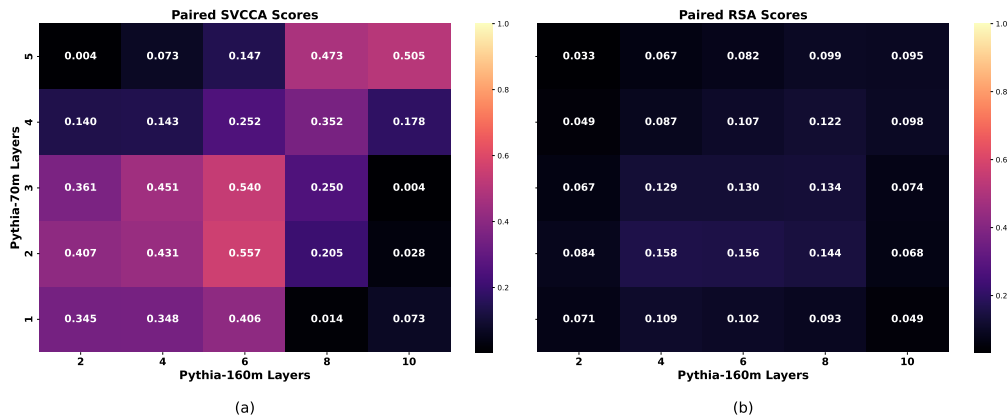


Figure 16: (a) SVCCA 1-1 paired scores of Eleuther’s 32k SAEs trained on Pythia-160m vs on Pythia-70m. (b) RSA 1-1 paired scores of the SAEs. The dataset activations were obtained using 40k tokens from the RedPajamas dataset.

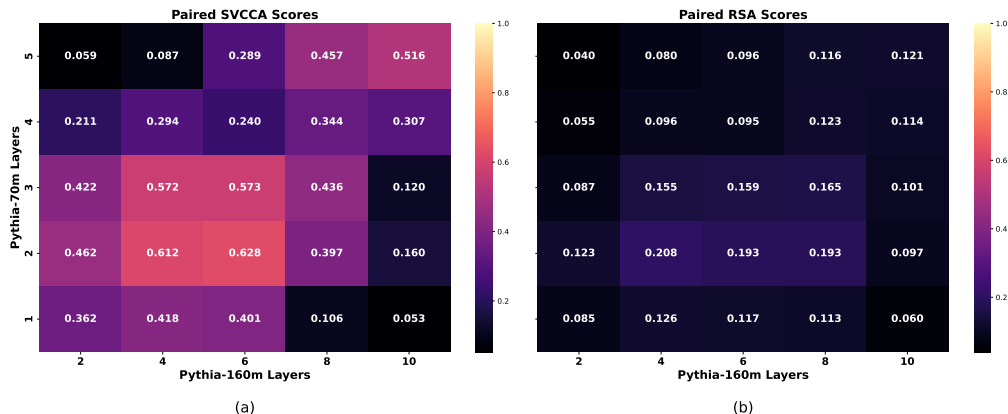


Figure 17: (a) SVCCA 1-1 paired scores of Eleuther’s 32k SAEs trained on Pythia-160m vs on Pythia-70m. (b) RSA 1-1 paired scores of the SAEs. The dataset activations were obtained using 40k tokens from the OpenWebText dataset.

G.2 COMPARING MORE DATA TO OBTAIN ACTIVATIONS

Figure 18 shows SVCCA Many-1 paired scores of SAEs for layers in Pythia-70m vs layers in Pythia-160m. This is run with 90k tokens, using 300 samples with a max sequence length of 300. Layer 3 appears to be an outlier, perhaps due to errors in feature matching. These results are similar to and consistent with the results of Figure 20, suggesting that other method is not heavily dependent on the number of tokens used to obtain activations.

H UNIVERSAL VS TRUE FEATURES

Our definition of universal features is based on Claim 3 of "Zoom In: An Introduction to Circuits", which defines universality as studying the extent to which analogous features and circuits form across models and tasks (Olah et al., 2020). Previous work has investigated similar claims by showing evidence for highly correlated neurons (Yosinski et al., 2014; Gurnee et al., 2024) and similar feature space representations at hidden layers (Kornblith et al., 2019; Klabunde et al., 2023). Using these definitions of universality, our results find both highly correlated features and similar feature representations in SAEs.

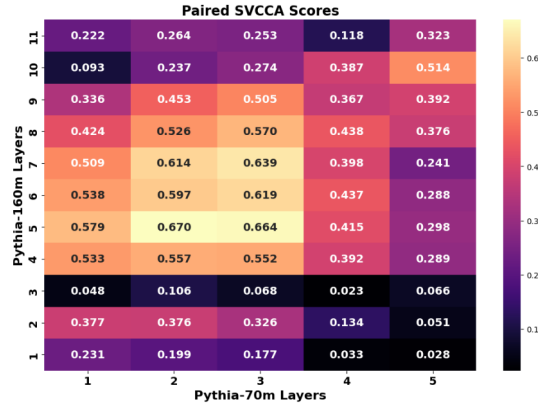


Figure 18: (a) SVCCA Many-1 paired scores of SAEs for layers in Pythia-70m vs layers in Pythia-160m. This is run with 90k tokens, using 300 samples with a max sequence length of 300. Layer 3 appears to be an outlier, perhaps due to errors in feature matching. This is consistent with Figure 20.

On the other hand, “true features” (Bricken et al., 2023) can be interpreted as atomic linear directions, such that activations are a linear combination of “true feature” directions (Till, 2023), though this term has not been formally defined yet. This definition for features imposes stricter requirements which do not just rely on high correlation and similar representations, but define “true features” as linear directions that model the same concepts, assuming they exist in ground truth. Previous work has shown that SAEs may capture ground truth features Sharkey et al. (2022), while recent research has provided evidence that SAE features are not atomic (Bussmann et al., 2024), which suggests SAEs may not be sufficient to capture “true features” if they exist.

Chughtai et al. (2023a) define universality in terms of *weak* and *strong* universality. Strong universality claims that models trained in similar ways will develop the same features and circuits, whereas weak universality argues that fundamental principles, such as similar functionalities, are learned across models, but their exact implementations may vary considerably. From this perspective, strong universality would correspond more with “true features”, while our paper would align closer to measuring weak universality in terms of similar feature space correlations. However, we also define *analogous feature universality* as a property between strong and weak universality which hypothesizes that while overall representations may greatly differ, there may be transformations that can be applied to a subset of these representations to better reveal their similarity.

The Importance of Analogous Features. While features across models may not capture the same ground truth feature representations, having analogous feature spaces could suggest that there may be transformations or mappings between the representation spaces of models which reveal their similarity. As such, this has implications for transfer learning and model stitching in which representations, including cross-layer circuits, from one model may be transferred to another (possibly larger) model through a mapping model. This may allow for functionality transfer. These studies may also have implications for furthering studies in neuroscience, as past research has been conducted on measuring the extent of alignment across biological and artificial neural networks (Goldstein et al., 2024), and previous work has also found high-low feature detectors in both vision models (Schubert et al., 2021) and mouse brains (Ding et al., 2023).

Currently, there are no standardized definitions for *analogous features*, though it may be possible to develop them. For instance, one possible way to better formalize a definition of analogous features would be along the lines of using a criteria akin to $(f \circ g)(x) = (h \circ f)(y)$, given that f is a mapping, while g and h are relations, such as distances, between points $x \in X$ and $y \in Y$ for spaces X and Y .

This paper seeks to measure the extent of universality in terms of “analogous features in representational space”, and unlike Huh et al. (2024), does not claim that models converge towards finding universal features. This follows previous papers which also measured the extent to which different neural networks learn the same representation (Wang et al., 2018a). We provide evidence that shows there are non-negligible signals of universality captured by subsets of SAE feature spaces across

models, but also claim that many feature space subsets in SAEs are dissimilar in terms of their representations and relations in feature space. Still, since this may be due to the limitations of SAEs in capturing features (Engels et al., 2024b), these results do not conclude that in these dissimilar areas, models do not share universal features, and further work must be done in this area to draw stronger conclusions.

Stated another way, this paper is not claiming that different SAEs consistently learn the same universal features captured by LLMs. Rather, it is claiming that LLMs learn weakly universal features, and that SAEs can capture not only these features, but their relations. However, one notable limitation is that SAEs cannot capture these features consistently.

I ILLUSTRATED STEPS OF COMPARISON METHOD

Figure 19 demonstrates steps 1 to 3 to carry out our similarity comparison experiments.

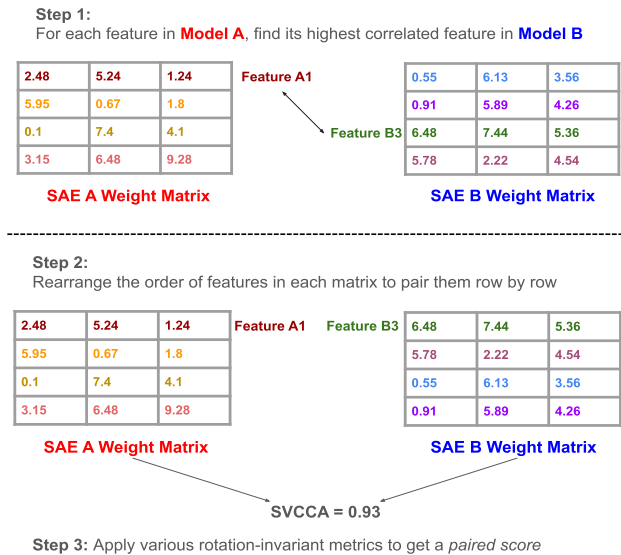


Figure 19: Steps to Main Results. We first find correlated pairs to solve neuron permutation, and then apply similarity metrics to solve latent space rotation issues.

J NOISE OF MANY-TO-1 MAPPINGS

Overall, we do not aim for mappings that uniquely pair every feature of both spaces as we hypothesize that it is unlikely that all the features are the same in each SAE; rather, we are looking for large subspaces where the features match by activations and we can map one subspace to another.

We hypothesize that these many-to-1 features may contribute a lot of noise to feature space alignment similarity, as information from a larger space (eg. a ball) is collapsed into a dimension with much less information (eg. a point). Thus, when we only include 1-1 features in our similarity scores, we receive scores with much less noise.

As shown in the comparisons of Figure 20 to Figure 21, we find the 1-1 feature mappings give slightly higher scores for many layer pairs, like for the SVCCA scores at L2 vs L3 for Pythia-70m vs Pythia-160m, though they give slightly lower scores for a few layer pairs, like for the SVCCA scores at L5 vs L4 for Pythia-70m vs Pythia-160m. Given that most layer pair scores are slightly higher, we use 1-1 feature mappings in our main text results.

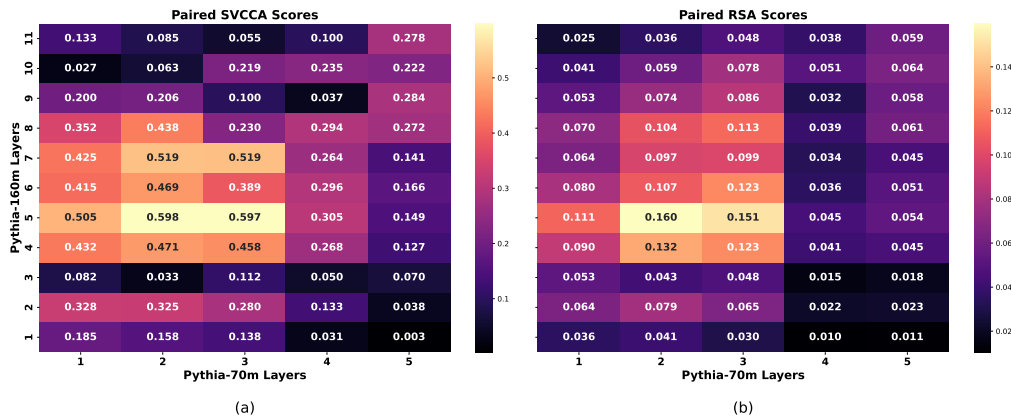


Figure 20: (a) SVCCA and (b) RSA **Many-to-1** paired scores of SAEs for layers in Pythia-70m vs layers in Pythia-160m. We note there appears to be an "anomaly" at L2 vs L3 with a low SVCCA score; we find that taking 1-1 features greatly increases this score from 0.03 to 0.35, as shown and explained in Figure 2.

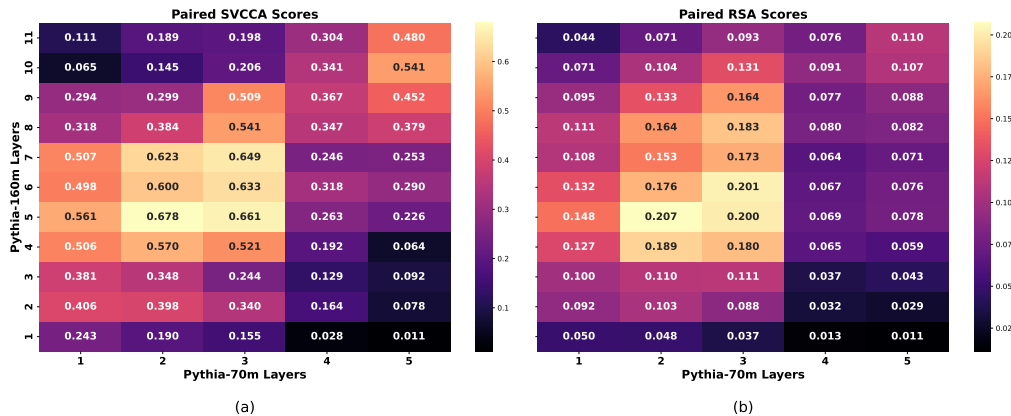


Figure 21: (a) SVCCA and (b) RSA **1-1** paired scores of SAEs for layers in Pythia-70m vs layers in Pythia-160m. Compared to Figure 20, some of the scores are slightly higher, and the SVCCA score at L2 vs L3 for 70m vs 160m is much higher. On the other hand, some scores are slightly lower, such as SVCCA at L5 vs L4 for 70m vs 160m. This is the same figure as Figure 2; it is shown here again for easier comparison to the Many-to-1 scores in Figure 20.

Additionally, we notice that for semantic subspace experiments, 1-1 gave vastly better scores than many-to-1. We hypothesize that this is because since these feature subspaces are smaller, the noise from the many-to-1 mappings have a greater impact on the score.

We also looked into using more types of 1-1 feature matching, such as pairing many-to-1 features with their "next highest" or using efficient methods to first select the mapping pair with the highest correlation, taking those features off as candidates for future mappings, and continuing this for the next highest correlations. This also appeared to work well, though further investigation is needed. More analysis can also be done for mapping one feature from SAE A to many features in SAE B.

K NOISE OF NON-CONCEPT FEATURE PAIRINGS

We define "non-concept features" as features which are not modeling specific concepts that can be mapped well across models. Their highest activations are on new lines, spaces, punctuation, and EOS tokens. As such, they may introduce noise when computing similarity scores, as their removal appears to greatly improve similarity scores. We hypothesize that one reason they introduce noise is that these

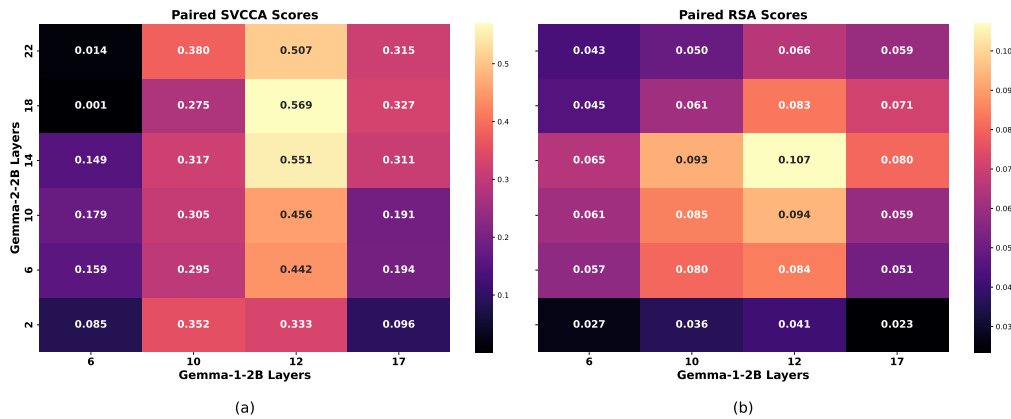


Figure 22: (a) SVCCA and (b) RSA **Many-to-1** paired scores of SAEs for layers in Gemma-1-2B vs layers in Gemma-2-2B. We obtain similar scores compared to the 1-1 paired scores in Figure 3.

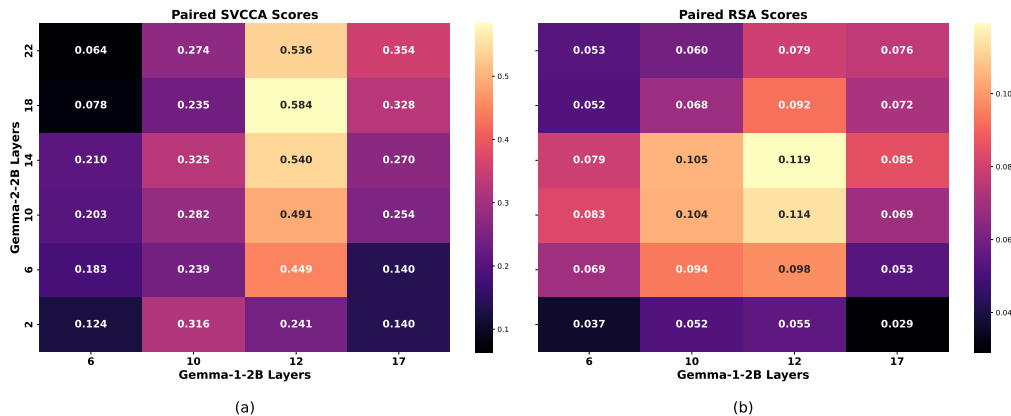


Figure 23: (a) SVCCA and (b) RSA **1-1** paired scores of SAEs for layers in Gemma-1-2B vs layers in Gemma-2-2B. Compared to Figure 22, some of the scores are slightly higher, while some are slightly lower. This is the same figure as Figure 3; it is shown here again for easier comparison to the Many-to-1 scores in Figure 20.

could be tokens that aren't specific to concepts, but multiple concepts. More specifically, since tokens are context dependent to a model, as information propagates through layers, the activations at a token position can aggregate information about that position's neighbors. Therefore, it is possible that these features are not "noisy" features, but are capturing concepts which are not represented well purely by activation correlation based on highest activating positions, and thus they are not well matched via activation correlation.

For instance, say feature X from model A fires highly on "!" in the sample "I am BOB!", while feature Y from model B fires highly on "!" in the sample, "that cat ate!"

A feature X that activates on "!" in "BOB!" may be firing for names, while a feature Y that activates on "!" in "ate!" may fire on food-related tokens. As such, features activating on non-concept features are not concept specific, and we could map a feature firing on names to a feature firing on food. We call these possibly "incoherent" mappings "non-concept mappings". By removing non-concept mappings, we show that SAEs reveal highly similar feature spaces.

A second hypothesis is that there are not diverse enough tokens to allow features to fire on what they should fire on. As such, providing more data to obtain correlations may allow these features to activate on more concepts, and thus be matched more accurately.

We filter "non-concept features" that fire, for at least one of their top 5 dataset examples, on a "non-concept" keyword. The list of "non-concept" keywords we use is given below:

- `\n`
- `\n`
- (empty string)
- (space)
- `.`
- `,`
- `!`
- `?`
- `-`
- respective padding token of tokenizer (`<bos>`, `<|endoftext|>`, etc.)

There may exist other non-concept features that we did not filter, such as colons, brackets and carats. We do not include arithmetic symbols, as those are domain specific to specific concepts. Additionally, we have yet to perform a detailed analysis on which non-concept features influence the similarity scores more than others; this may be done in future work.

L CONCEPT CATEGORIES LIST AND FURTHER ANALYSIS

The keywords used for each concept group for the semantic subspace experiments are given in Table 4. We generate these keywords using GPT-4 Bubeck et al. (2023) using the prompt "give a list of N single token keywords as a python list that are related to the concept of C", such that N is a number (we use N=50 or 100) and C is a concept like Emotions. We then manually filter these lists to avoid using keywords which have meanings outside of the concept group (eg. "even" does not largely mean "divisible by two" because it is often used to mean "even if..."). We also aim to select keywords which are single-tokens with no spaces, and are case-insensitive.⁴

When searching for keyword matches from each feature's list of top 5 highest activating tokens, we use keyword matches that avoid features with dataset samples which use the keywords in compound words. For instance, when searching for features that activate on the token "king" from the People/Roles concept, we avoid using features that activate on "king" when "king" is a part of the word "seeking", as that is not related to the People/Roles concept.

We perform interpretability experiments to check which keywords of the features kept are activated on. We find that for many feature pairs, they activate on the same keyword and are monosemantic. Most keywords in each concept group are not kept. Additionally, for the layer pairs we checked on, after filtering there were only a few keywords that multiplied features fired on. This shows that the high similarity is not because the same keyword is over-represented in a space.

For instance, for Layer 3 in Pythia-70m vs Layer 5 in Pythia-160m, and for the concept category of Emotions, we find which keywords from the category appear in the top 5 activating tokens of each of the Pythia-70m features from the 24 feature mappings described in Table 1. We only count a feature if it appears once in the top 5 of a feature's top activating tokens; if three out of five of a feature's top activating tokens are "smile", then smile is only counted once. The results for Models A and B are given in Table 3. Not only are their counts similar, indicating similar features, but there is not a great over-representation of features. There are a total of 24 features, and a total of 25 keywords (as some features can activate on multiple keywords in their top 5). We note that even if a feature fires for a keyword does not mean that feature's purpose is only to "recognize that keyword", as dataset examples as just one indicator of what a feature's purpose is (which still can have multiple, hard-to-interpret purposes).

However, as there are many feature pairs, we did not perform a thorough analysis of this yet, and thus did not include this analysis in this paper. We also check this in LLMs, and find that the majority of

⁴However, not all the tokens in the Table 4 are single token.

Table 3: Count of Model A vs Model B features with keywords from the Emotion category in the semantic subspace found in Table 1.

Model A		Model B	
Keyword	Count	Keyword	Count
free	4	free	5
pain	4	pain	4
smile	3	love	3
love	2	hate	2
hate	2	calm	2
calm	2	smile	2
sad	2	kind	1
kind	1	shy	1
shy	1	doubt	1
doubt	1	trust	1
trust	1	peace	1
peace	1	joy	1
joy	1	sad	1

LLM neurons are polysemantic. We do not just check the top 5 dataset samples for LLM neurons, but the top 90, as the SAEs have an expansion factor that is around 16x or 32x bigger than the LLM dimensions they take in as input.

Calendar is a subset of Time, removing keywords like “after” and “soon”, and keeping only “day” and “month” type of keywords pertaining to dates.

Future work can test on several groups of unrelated keywords, manually inspecting to check that each word belongs to its own category. Another test to run is to compare the score of a semantic subspace mapping to a mean score of subspace mapping of the same number of correlated features, using the correlation matrix of the entire space. Showing that these tests result in high p-values will provide more evidence that selecting any subset of correlated features is not enough, and that having the features be semantically correlated with one another yields higher similarity.

M ADDITIONAL RESULTS FOR PYTHIA AND GEMMA

As shown in Figure 24 for Pythia and Figure 25 for Gemma, we also find that mean activation correlation does not always correlate with the global similarity metric scores. For instance, a subset of feature pairings with a moderately high mean activation correlation (eg. 0.6) may yield a low SVCCA score (eg. 0.03).

The number of features after filtering non-concept features and many-to-1 features are given in Tables 5 and 6. The number of features after filtering non-concept features and many-to-1 features are given in Tables 7 and 8.

Table 4: Keywords Organized by Category

Category	Keywords
Time	day, night, week, month, year, hour, minute, second, now, soon, later, early, late, morning, evening, noon, midnight, dawn, dusk, past, present, future, before, after, yesterday, today, tomorrow, next, previous, instant, era, age, decade, century, millennium, moment, pause, wait, begin, start, end, finish, stop, continue, forever, constant, frequent, occasion, season, spring, summer, autumn, fall, winter, anniversary, deadline, schedule, calendar, clock, duration, interval, epoch, generation, period, cycle, timespan, shift, quarter, term, phase, lifetime, timeline, delay, prompt, timely, recurrent, daily, weekly, monthly, yearly, annual, biweekly, timeframe
Calendar	day, night, week, month, year, hour, minute, second, morning, evening, noon, midnight, dawn, dusk, yesterday, today, tomorrow, decade, century, millennium, season, spring, summer, autumn, fall, winter, calendar, clock, daily, weekly, monthly, yearly, annual, biweekly, timeframe
People/Roles	man, girl, boy, kid, dad, mom, son, sis, bro, chief, priest, king, queen, duke, lord, friend, clerk, coach, nurse, doc, maid, clown, guest, peer, punk, nerd, jock
Nature	tree, grass, stone, rock, cliff, hill, dirt, sand, mud, wind, storm, rain, cloud, sun, moon, leaf, branch, twig, root, bark, seed, tide, lake, pond, creek, sea, wood, field, shore, snow, ice, flame, fire, fog, dew, hail, sky, earth, glade, cave, peak, ridge, dust, air, mist, heat
Emotions	joy, glee, pride, grief, fear, hope, love, hate, pain, shame, bliss, rage, calm, shock, dread, guilt, peace, trust, scorn, doubt, hurt, wrath, laugh, cry, smile, frown, gasp, blush, sigh, grin, woe, spite, envy, glow, thrill, mirth, bored, cheer, charm, grace, shy, brave, proud, glad, mad, sad, tense, free, kind
MonthNames	January, February, March, April, May, June, July, August, September, October, November, December
Countries	USA, Canada, Brazil, Mexico, Germany, France, Italy, Spain, UK, Australia, China, Japan, India, Russia, Korea, Argentina, Egypt, Iran, Turkey
Biology	gene, DNA, RNA, virus, bacteria, fungus, brain, lung, blood, bone, skin, muscle, nerve, vein, organ, evolve, enzyme, protein, lipid, membrane, antibody, antigen, ligand, substrate, receptor, cell, chromosome, nucleus, cytoplasm

Table 5: Number of Features in each Layer Pair Mapping after filtering Non-Concept Features for Pythia-70m (cols) vs Pythia-160m (rows) out of a total of 32768 SAE features in both models.

Layer	1	2	3	4	5
1	23600	21423	26578	19696	19549
2	16079	14201	17578	12831	12738
3	7482	7788	7841	7017	6625
4	12756	11195	13349	9019	9357
5	7987	6825	8170	5367	5624
6	10971	9578	10937	8099	8273
7	15074	12988	16326	12720	12841
8	14445	12580	15300	11779	11942
9	13320	11950	14338	11380	11436
10	9834	8573	9742	7858	8084
11	6936	6551	7128	5531	6037

Table 6: Number of **1-1** Features in each Layer Pair Mapping after filtering Non-Concept Features for Pythia-70m (cols) vs Pythia-160m (rows) out of a total of 32768 SAE features in both models.

Layer	1	2	3	4	5
1	7553	5049	5853	3244	3115
2	6987	4935	5663	3217	3066
3	4025	3152	3225	2178	1880
4	6649	5058	6015	3202	3182
5	5051	4057	4796	2539	2596
6	5726	4528	5230	3226	3031
7	7017	5659	6762	4032	3846
8	6667	5179	6321	3887	3808
9	6205	4820	5773	3675	3682
10	4993	3859	4602	3058	3356
11	3609	2837	3377	2339	2691

Table 7: Number of Features in each Layer Pair Mapping after filtering Non-Concept Features for Gemma-1-2B (cols) vs Gemma-2-2B (rows) out of a total of 16384 SAE features in both models.

Layer	6	10	12	17
2	8926	8685	8647	4816
6	4252	4183	4131	2474
10	6458	6320	6277	3658
14	4213	4208	4214	2672
18	3672	3679	3771	2515
22	4130	4100	4168	3338

Table 8: Number of **1-1** Features in each Layer Pair Mapping after filtering Non-Concept Features for Gemma-1-2B (cols) vs Gemma-2-2B (rows) out of a total of 16384 SAE features in both models.

Layer	6	10	12	17
2	3427	3874	3829	1448
6	3056	3336	3261	1266
10	4110	4650	4641	1616
14	2967	3524	3553	1414
18	2636	3058	3239	1543
22	2646	3037	3228	1883

Table 9: RSA scores and random mean results for 1-1 semantic subspaces of L3 of Pythia-70m vs L5 of Pythia-160m. P-values are taken for 1000 samples in the null distribution.

Concept Subspace	Number of 1-1 Features	Paired Mean	Random Shuffling Mean	p-value
Time	228	0.10	0.00	0.00
Calendar	126	0.09	0.00	0.00
Nature	46	0.22	0.00	0.00
MonthNames	32	0.76	0.00	0.00
Countries	32	0.10	0.00	0.03
People/Roles	31	0.18	0.00	0.01
Emotions	24	0.46	0.00	0.00

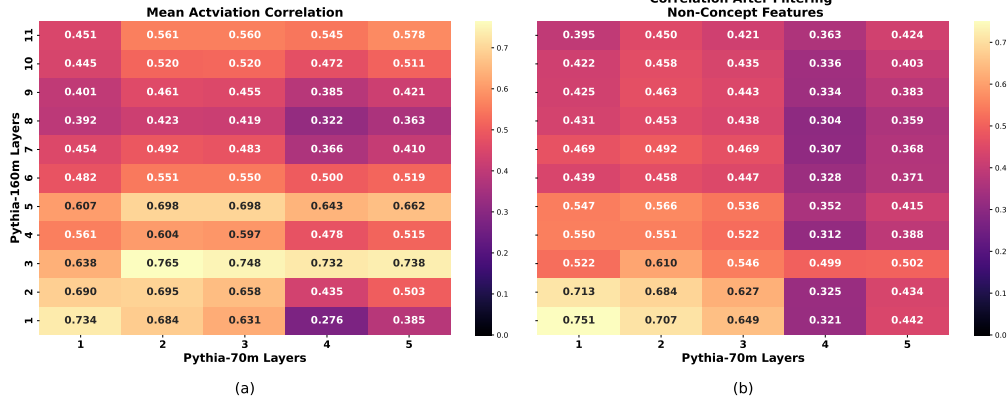


Figure 24: Mean Activation Correlation before (a) and after (b) filtering non-concept features for Pythia-70m vs Pythia-160m. We note these patterns are different from those of the SVCCA and RSA scores in Figure 20, indicating that these three metrics each reveal different patterns not shown by other metrics.

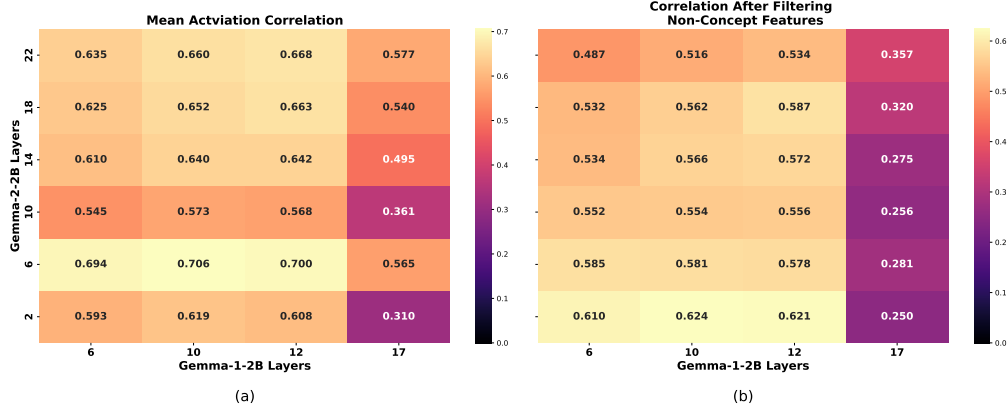


Figure 25: Mean Activation Correlation before (a) and after (b) filtering non-concept features for Gemma-1-2B vs Gemma-2-2B. We note these patterns are different from those of the SVCCA and RSA scores in Figure 22, indicating that these three metrics each reveal different patterns not shown by other metrics.

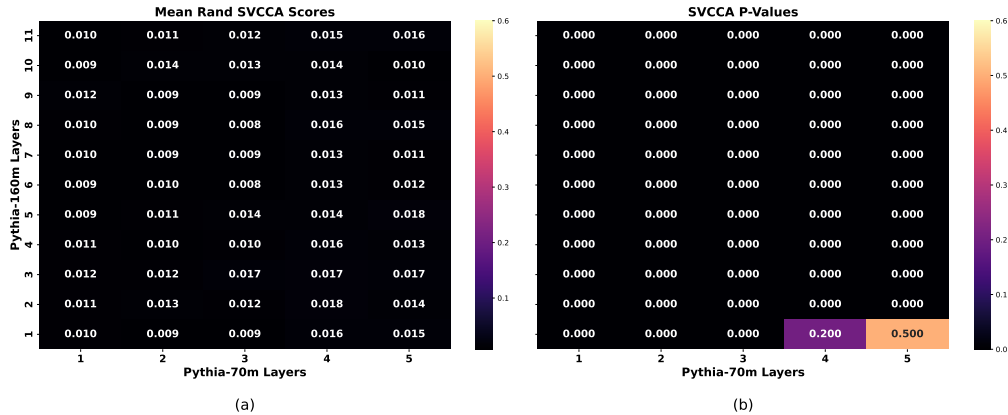


Figure 26: Mean Randomly Paired SVCCA scores and P-values of SAEs for layers in Pythia-70m vs Pythia-160m. Compared to Paired Scores in Figure 20, these are all very low.

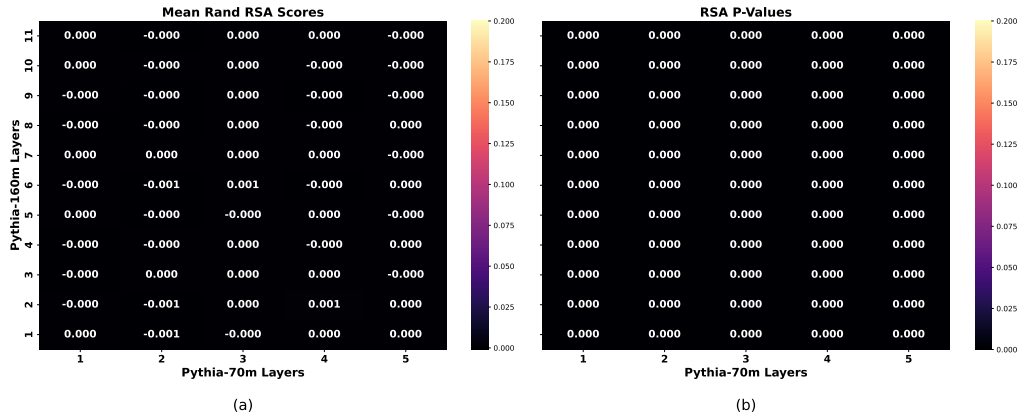


Figure 27: Mean Randomly Paired RSA scores and P-values of SAEs for layers in Pythia-70m vs Pythia-160m. Compared to Paired Scores in Figure 20, these are all very low.

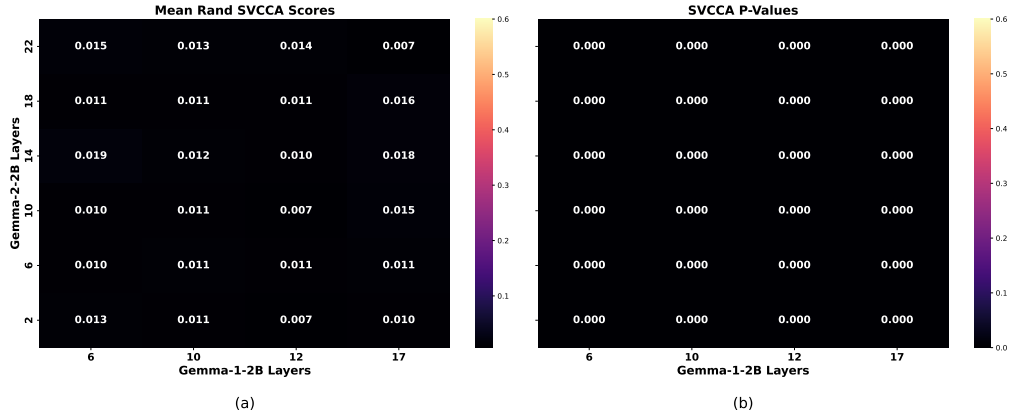


Figure 28: Mean Randomly Paired SVCCA scores and P-values of SAEs for layers in Gemma-1-2B vs layers in Gemma-2-2B. Compared to Paired Scores in Figure 22, these are all very low.

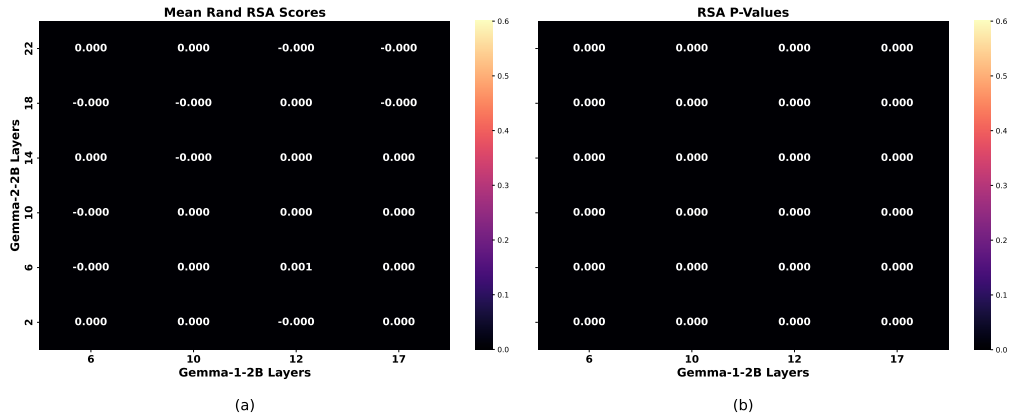


Figure 29: Mean Randomly Paired RSA scores and P-values of SAEs for layers in Gemma-1-2B vs layers in Gemma-2-2B. Compared to Paired Scores in Figure 22, these are all very low.

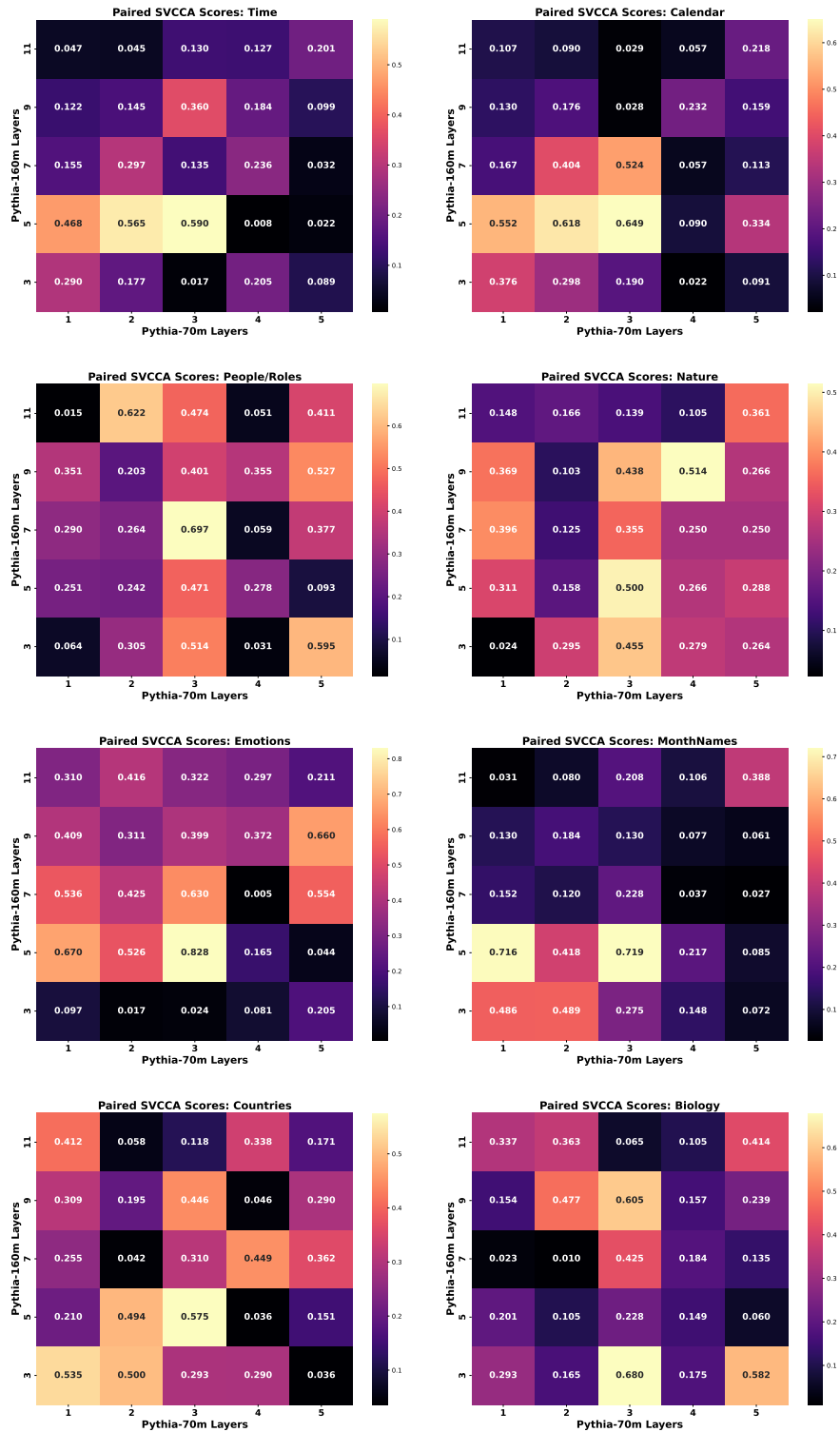


Figure 30: 1-1 Paired SVCCA scores of SAEs for layers in Pythia-70m vs layers in Pythia-160m for Concept Categories. Middle layers appear to be the most similar with one another.

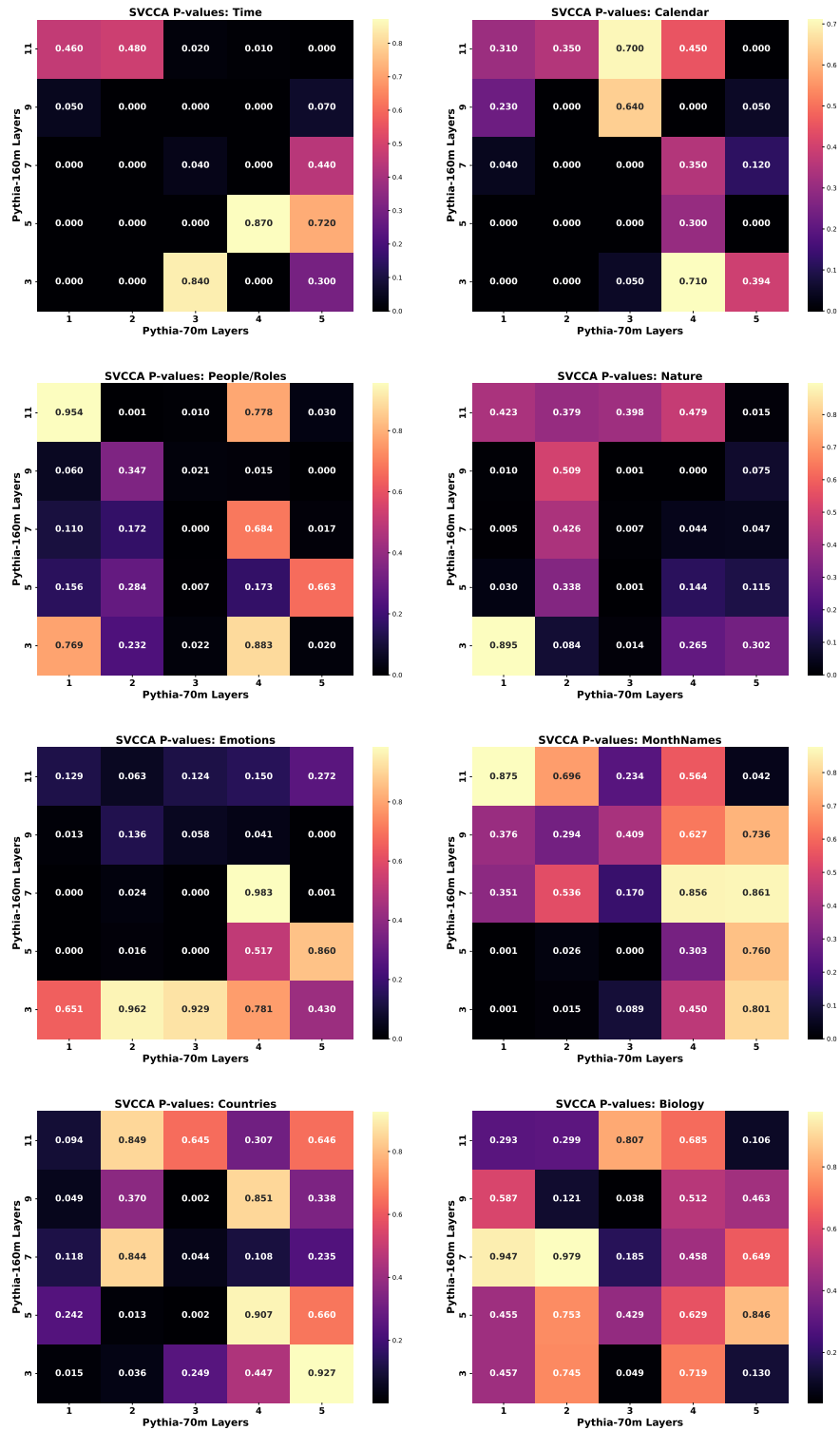


Figure 31: 1-1 SVCCA p-values of SAEs for layers in Pythia-70m vs layers in Pythia-160m for Concept Categories. A lower p-value indicates more statistically meaningful similarity.

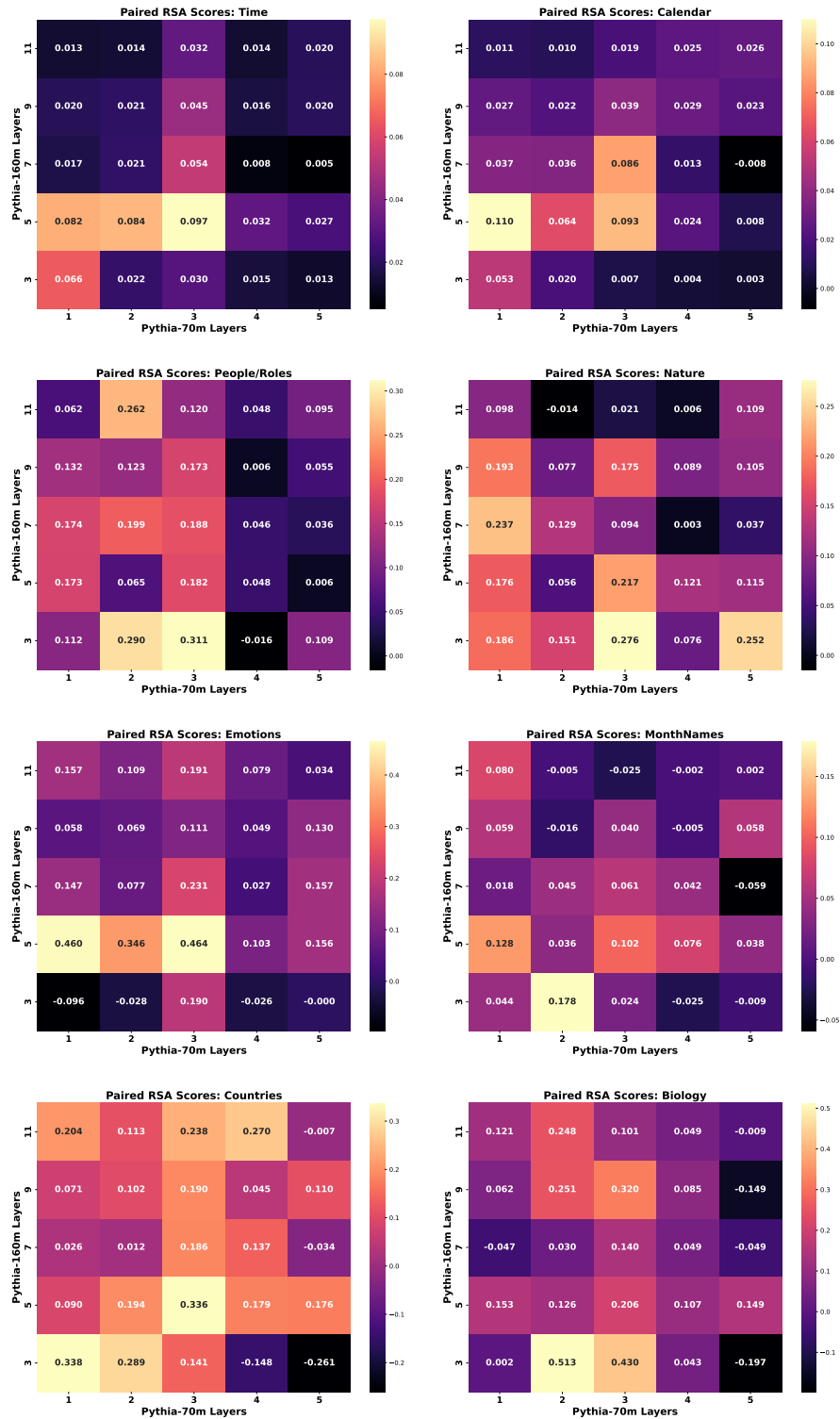


Figure 32: 1-1 Paired RSA scores of SAEs for layers in Pythia-70m vs layers in Pythia-160m for Concept Categories. Middle layers appear to be the most similar with one another.

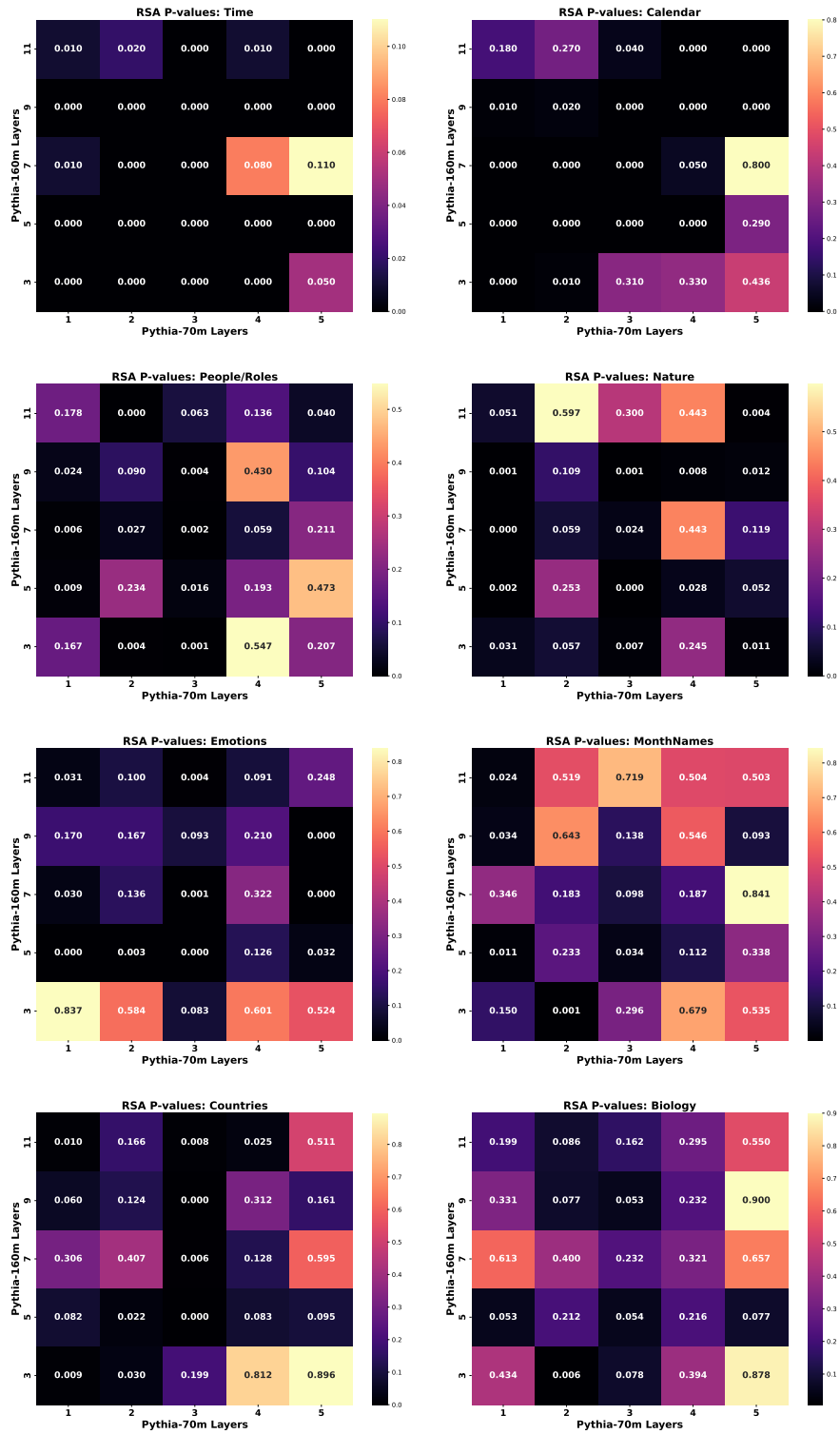


Figure 33: 1-1 RSA p-values of SAEs for layers in Pythia-70m vs layers in Pythia-160m for Concept Categories. A lower p-value indicates more statistically meaningful similarity.

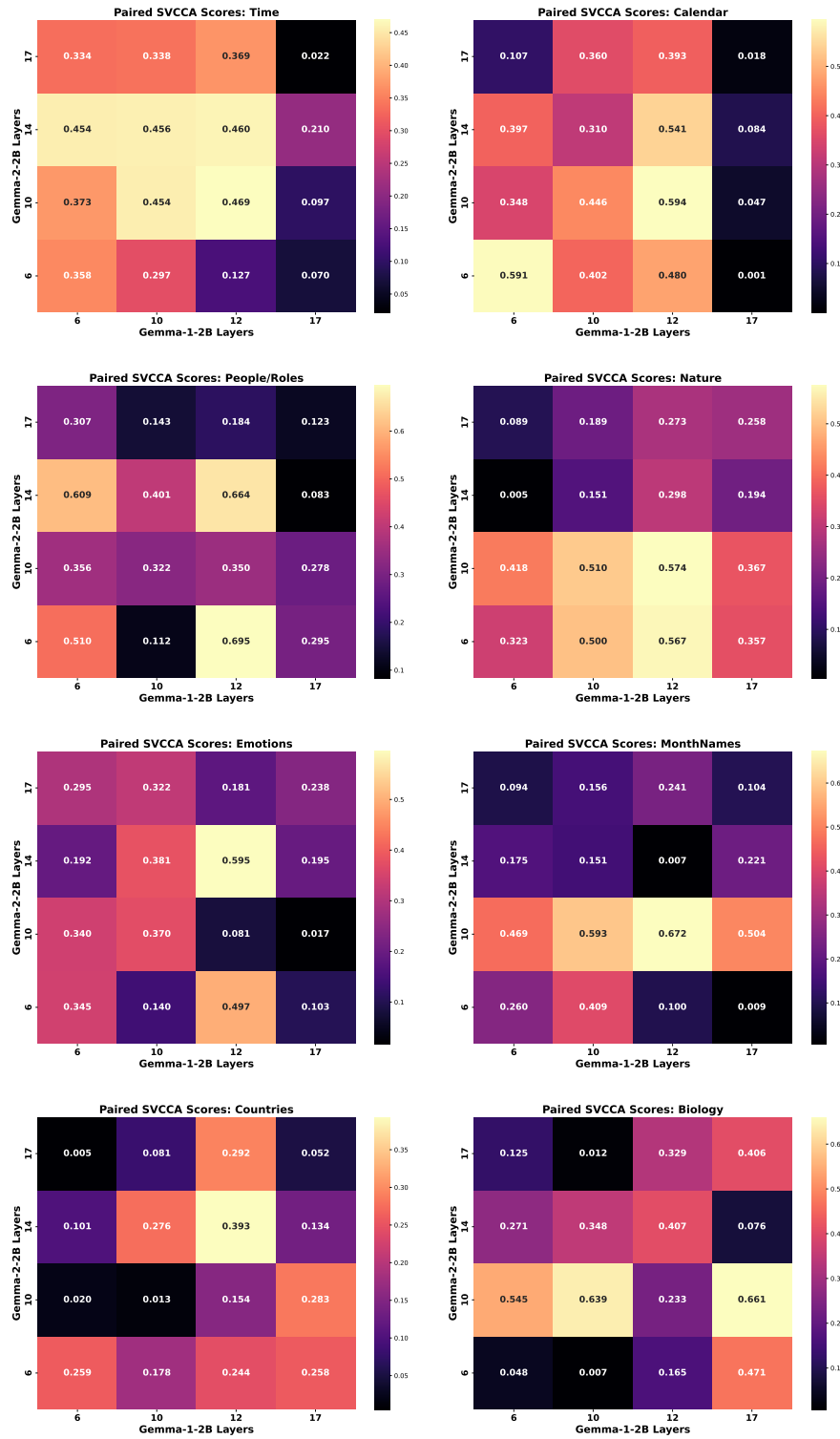


Figure 34: 1-1 Paired SVCCA scores of SAEs for layers in Gemma-1-2b vs layers in Gemma-2-2b for Concept Categories. Middle layers appear to be the most similar with one another.

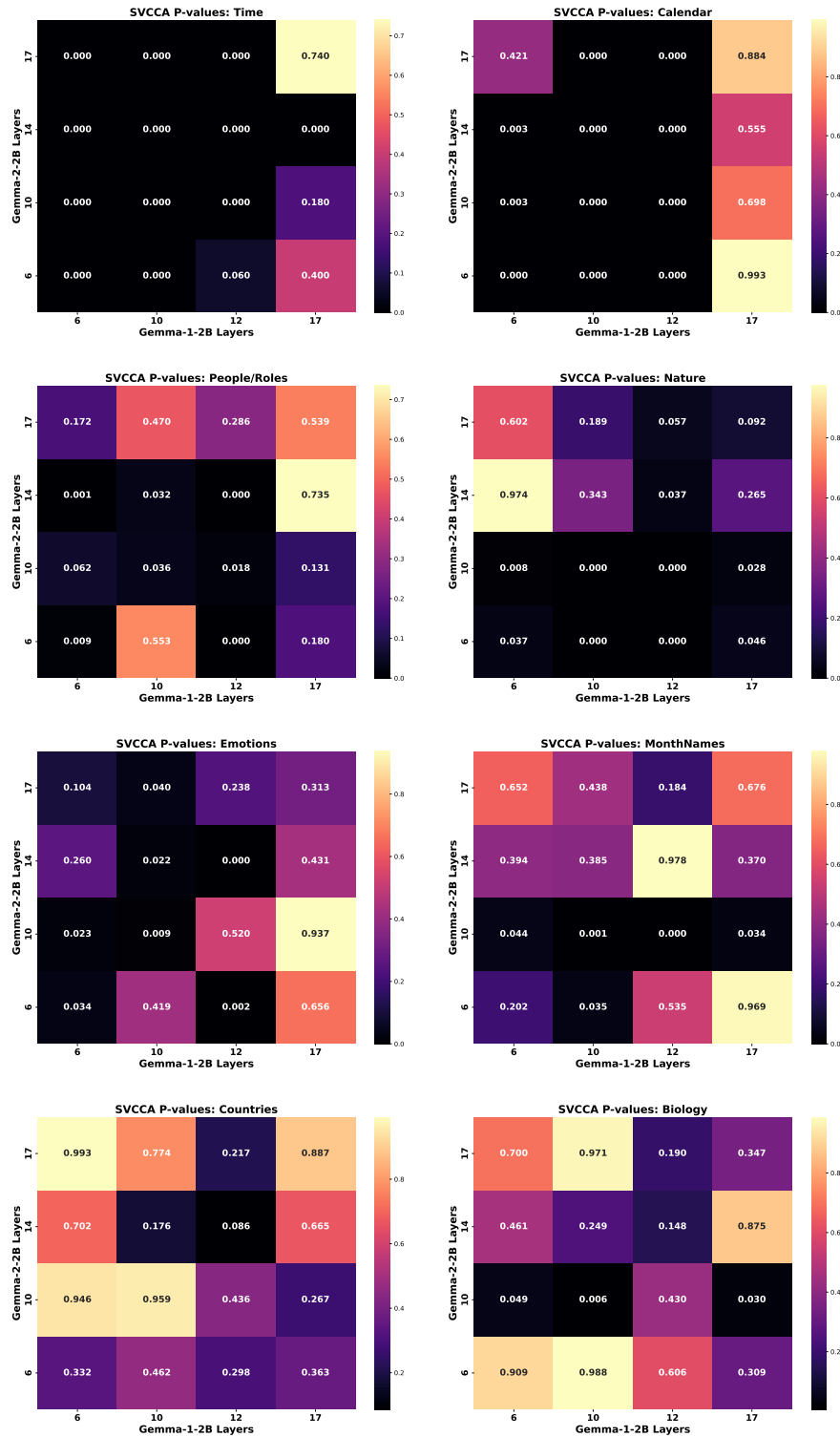


Figure 35: 1-1 SVCCA p-values of SAEs for layers in Gemma-1-2b vs layers in Gemma-2-2b for Concept Categories. A lower p-value indicates more statistically meaningful similarity.

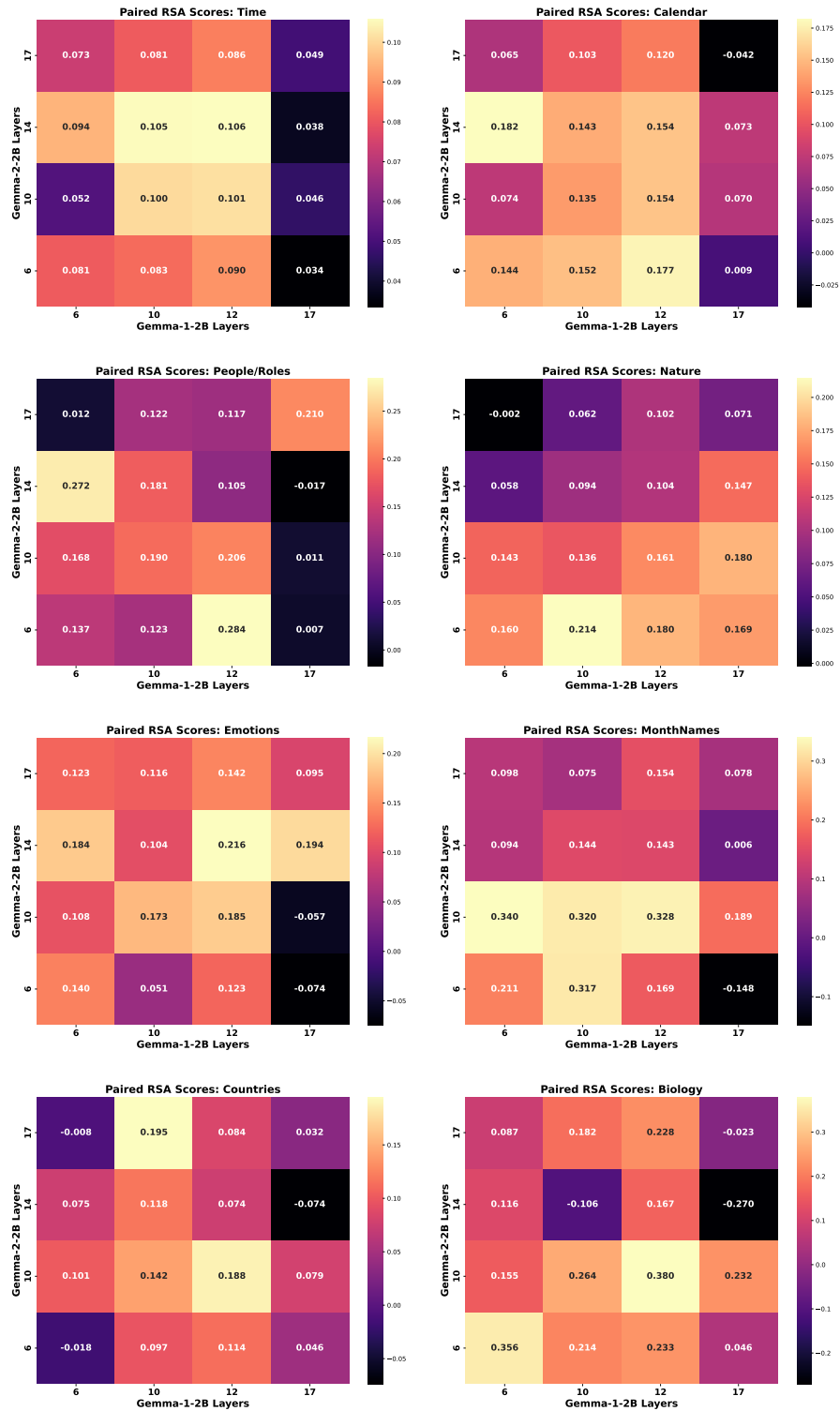


Figure 36: 1-1 Paired RSA scores of SAEs for layers in Gemma-1-2b vs layers in Gemma-2-2b for Concept Categories. Middle layers appear to be the most similar with one another.

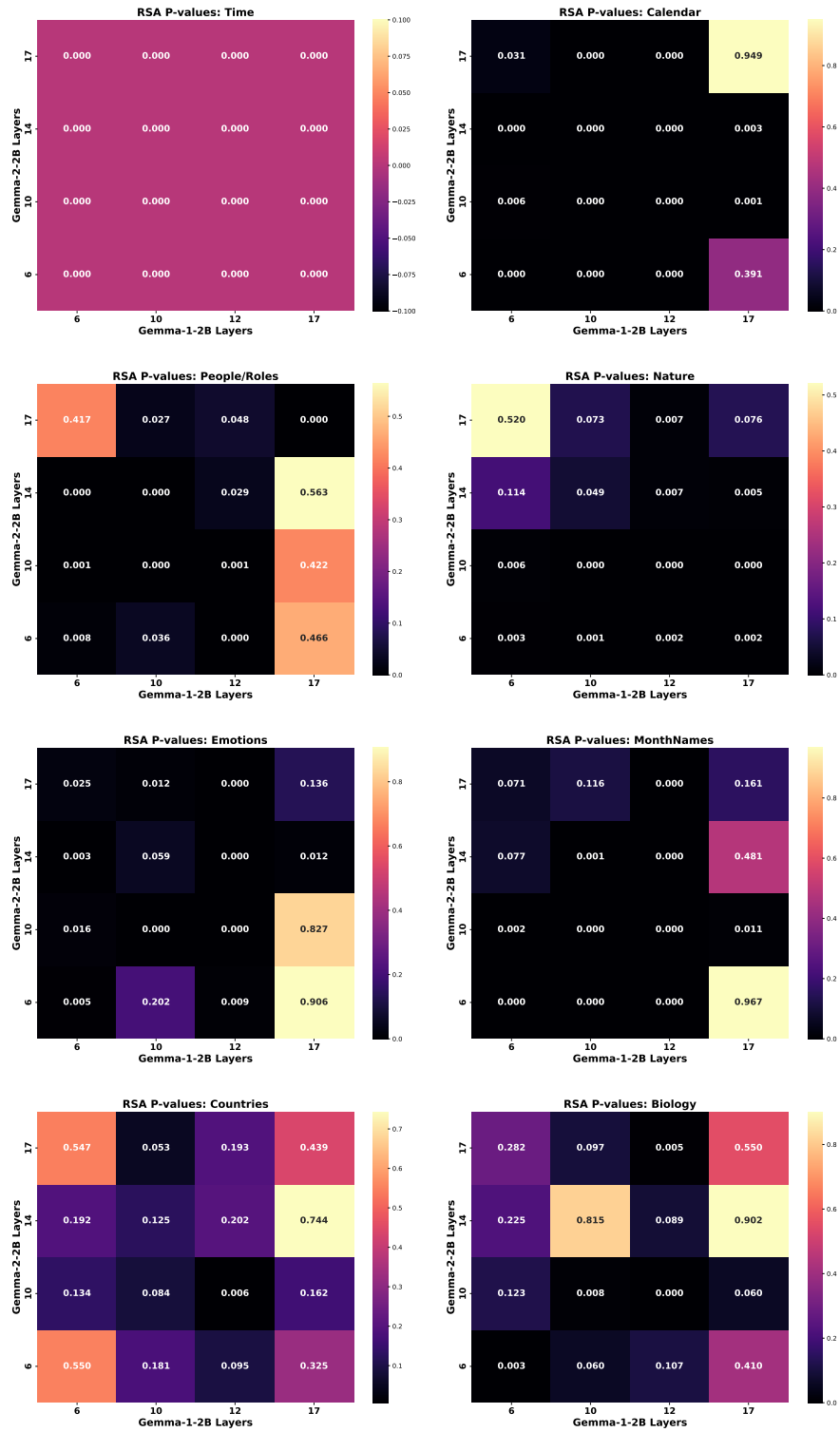


Figure 37: 1-1 RSA p-values of SAEs for layers in Gemma-1-2b vs layers in Gemma-2-2b for Concept Categories. A lower p-value indicates more statistically meaningful similarity.